Synthesis and evaluation of butein derivatives for in vitro and in vivo inflammatory response suppression in lymphedema

Kangsan Roh, Jung-hun Lee, Hee Kang, Kyewon Park, Youngju Song, Sukchan Lee, Jin-Mo Ku

PII: S0223-5234(20)30249-X

DOI: https://doi.org/10.1016/j.ejmech.2020.112280

Reference: EJMECH 112280

To appear in: *European Journal of Medicinal Chemistry*

Received Date: 31 December 2019

Revised Date: 26 March 2020

Accepted Date: 26 March 2020

Please cite this article as: K. Roh, J.-h. Lee, H. Kang, K. Park, Y. Song, S. Lee, J.-M. Ku, Synthesis and evaluation of butein derivatives for in vitro and in vivo inflammatory response suppression in lymphedema, *European Journal of Medicinal Chemistry* (2020), doi: https://doi.org/10.1016/j.ejmech.2020.112280.

GRAPHICAL ABSTRACT

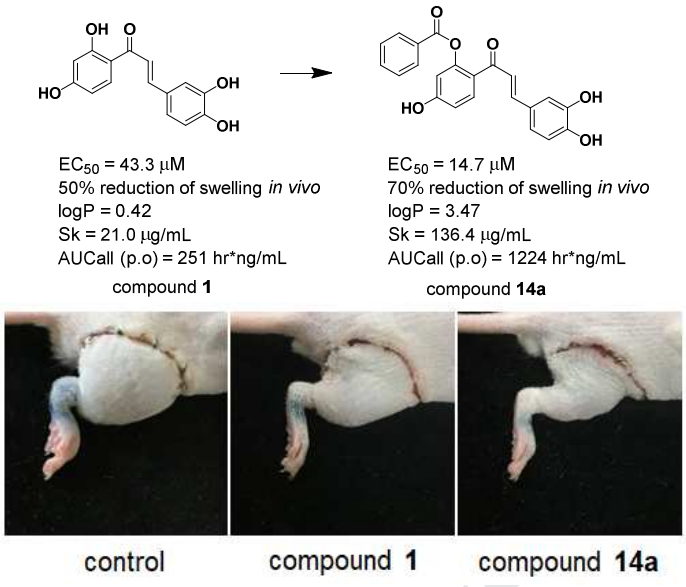

Synthesis and evaluation of butein derivatives for in vitro and in vivo inflammatory response suppression in lymphedema

Kangsan Roh[2†], Jung-hun Lee[1†], Hee Kang[3†], Kyewon Park[4], Youngju Song[5], Sukchan Lee[2], Jin-Mo Ku[1]**

[1] Bio-Center, Gyeonggido Business & Science Accelerator, 147 Gwanggyo-ro, Suwon 16229, Republic of Korea

[2] Department of Integrative Biotechnology, Sungkyunkwan University, Suwon 16419, Republic of Korea

[3] Humanitas College, Kyung Hee University, Yongin 17104, Republic of Korea

[4] Department of Food Science and Biotechnology, Sungkyunkwan University, Suwon 16419, Republic of Korea

[5] Department of Biomedical Science and Technology, Graduate School, Kyung Hee University, Seoul 02447, Republic of Korea

* To whom correspondence should be addressed.

For J.-M. Ku: phone, 82-31-888-6987; fax, 82-31-888-6979; e-mail, medichem@gbsa.or.kr

For S. Lee: phone, 82-31-290-7866; e-mail, cell4u@skku.edu

* Authors for co-correspondence

† These authors contributed equally to this work and should be considered co-first authors.

KEYWORDS: Acquired lymphedema, inflammation, chalcones, therapeutic agent

GRAPHICAL ABSTRACT

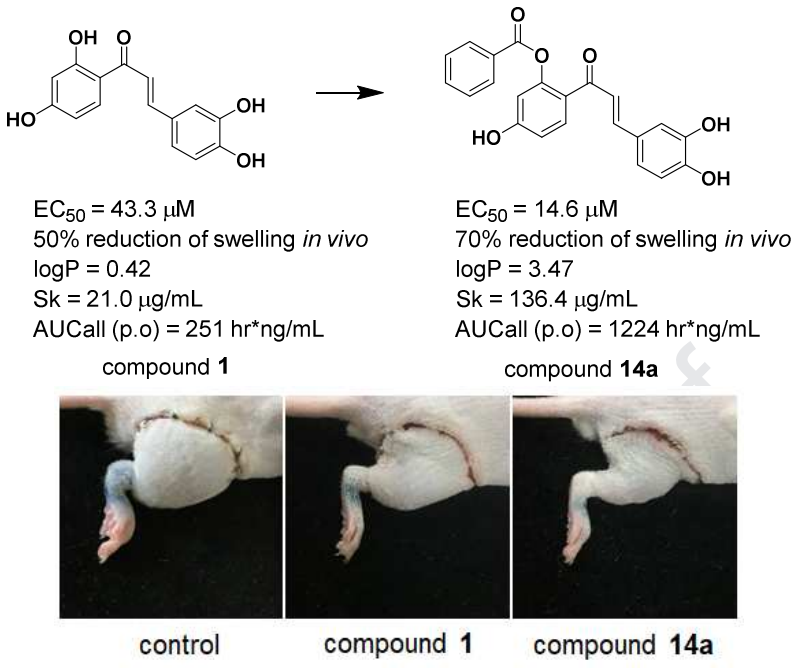

ABSTRACT:

Herein, we demonstrate that butein (**1**) can prevent swelling in a murine lymphedema model by suppressing tumor necrosis factor α (TNF-α) production. Butein derivatives were synthesized and evaluated to identify compounds with in vitro anti-inflammatory activity. Among them, 20 μM of compounds **7j**, **7m**, and **14a** showed 50% suppression of TNF-α production in mouse peritoneal macrophages after lipopolysaccharide stimulation. Compound **14a**, exhibited the strongest potency with an in vitro IC_{50} of 14.6 μM and suppressed limb volume by 70% in a murine lymphedema model. The prodrug strategy enabled a six-fold increase in kinetic solubility of compound **1** and five-fold higher levels of active metabolite in the blood for compound **14a** via oral administration in the pharmacokinetics study. We

suggest that the compound **14a** could be developed as a potential therapeutic agent targeting anti-inflammatory activity to alleviate lymphedema progression.

INTRODUCTION

Lymphedema occurs when an abnormality or injury in the lymphatic system blocks adequate lymph drainage from the arm or leg. Lymphedema is classified into congenital lymphedema and acquired lymphedema.[1] Acquired lymphedema is often caused by cancer treatments, such as surgery, radiation, and chemotherapy, or after physical trauma or infections.[2] The manifestations of lymphedema include swelling, reduced functionality of the limbs, and subsequent secondary infections, lead to psychological distress and detrimental effects on social and work life.[3] Currently, there is no therapeutic agent that can inhibit lymphedema progression or alleviate its symptoms. Complete decongestive therapy (CDT), a physiotherapeutic approach, is commonly accepted as the primary treatment for lymphedema as it aims to decrease fluid accumulation.[4]

Although many efforts have been underway to find new targets for systemically controlling lymphedema, its molecular mechanisms are not clearly defined. It is known that the accumulation of interstitial fluid leads to inflammation, fat deposition, and fibrosis.[5] Many reports have indicated that immune responses related to inflammatory cell infiltration play a critical role in the pathophysiology of lymphedema. [6] Upregulation of inflammatory genes have been observed in both murine models and patients–with lymphedema.[7,8] Based on previous studies, inflammatory responses were necessary for lymphedema formation during adipose tissue inflammation in obese mouse models.[9,10] Swapna et al. also revealed that the

proinflammatory responses caused by macrophage infiltration can be significantly affected in response to lymphedema.[11] Patients using CDT showed reduced expression of tumor necrosis factor(TNF)-α and other proinflammatory mediators.[12] These data suggest that anti-inflammatory agents can be potential targets for alleviating lymphedema progression.

Several anti-inflammatory compounds have been tried in experimental lymphedema models and have shown promising effects. Ketoprofen, a commonly used nonsteroidal anti-inflammatory drug (NSAID), was subcutaneously applied to a murine tail and it ameliorated swelling and other pathologic symptoms.[13] Tacrolimus, an anti-T-cell agent used for chronic cutaneous inflammation and fibrosis, was successful in preventing and improving lymphedema in the above-mentioned lymphedema model.[14] Although ketoprofen and tacrolimus are currently being assessed as novel clinical lymphedema therapies, their potential toxicities may limit their long-term use.

In our investigation into finding therapeutic candidates, we previously established a new lymphedema mouse model that mimics lymphedema in cancer patients by removing a superficial inguinal lymph node, a popliteal lymph node, a deep inguinal lymph node, and the femoral lymphatic vessel. Using the model, we found that Rhus verniciflua Stokes (RVS) ameliorated hind leg edema.[15] RVS extract contains several anti-inflammatory polyphenols, including sulfuretin and compound **1**. Compound **1** is more potent than other polyphenols, e.g., sulfuretin, in suppressing lipopolysaccharide (LPS)-induced nitrite and prostaglandin E_2 production in macrophages.[16] In addition to its anti-inflammatory activity, compound **1** can inhibit adipogenesis and fibrosis.[17,18] These properties prompted us to explore the systemic effect of compound **1** on lymphedema. At the same time, we attempted to optimize the chemical structure of compound **1** in order to improve in vitro and in vivo efficacy through structure-activity relationship (SAR) analysis. The goal was to produce a prodrug of

compound **1** to enhance the potency, solubility, permeability, and pharmacokinetic parameters, including half-life and pharmaceutically active levels in the blood.

RESULTS AND DISCUSSION

In Vitro and In Vivo Lead Compound Validation

As an initiative to find therapeutic candidates, our strategy is to choose a lead compound that can suppress TNF-α, the master inflammatory cytokine that is mainly produced by activated macrophages and recruit circulating neutrophils to injured tissue. Compound **1** was tested for its ability to inhibit the production of TNF-α in lipopolysaccharide (LPS)-stimulated macrophages. Compound **1** decreased TNF-α production by 10% at 20 μM and had a dose-dependent IC_{50} of 43.3 μM (supporting information 1A).

We verified that swelling of the affected limb decreased with oral administration of compound in a murine lymphedema model. The limb volume was reduced with compound **1** treatment on days three and seven post-surgery (supporting information 1B). Oral administration of compound **1** (200 mg/kg/d) caused dramatic suppression of lymphedema, reducing the volume by 41.6% (41.5 mm^2) compared with that of the untreated mouse (99 mm^2). H&E staining of the affected lower limb supported this finding (supporting information 1C). Thereby, we determined that compound **1** is a promising anti-inflammatory lead compound through in vitro and in vivo work, suggesting the need for further lead

optimization of compound **1** to improve the potency and efficacy via structure-activity relationship (SAR) studies.

Lead Optimization Through Chemical Modification and Anti-inflammatory Evaluation

Compound **1** exhibits poor water solubility (79 μM, 21.0 μg/mL), with a partition coefficient, (logP) of 0.42. In addition, it has low potency (IC_{50}, 43.3 μM) and insufficient efficacy, with only 21% inhibition at 20 μM in vitro, indicating that it is not a suitable candidate for evaluation in vivo. To address these deficiencies, we performed structure-activity-guided modifications of compound **1** to improve its physicochemical properties (solubility, logP) and pharmacokinetic parameters, including maximum concentration of a drug (Cmax), bioavailability (BA), half-life ($T_{1/2}$), and total concentration of the drug (area under curve, AUC) after oral administration.

Compound **1** is one of natural product which is structurally similar to isoliquiritigenin (**2**), echinatin (**3**), and licochalcone B (**4**), all of which have a chalcone backbone with phenols. . (Figure 1A). We compared the inhibitory effects of compounds **1** and **3** and ketoprofen at 20 μM on LPS-stimulated TNF-α production in macrophages and found a similar activity (Supporting information 2A). Ketoprofen had no effect in this model. Subsequently, we planned to modify the structure of compound **1** via structure-activity relationship studies by functional group interconversion to inhibit TNF-α production in macrophages.

Functional group modifications on each aromatic ring in sections A and B of compound **1** helped identify pharmacophores for biological activity (Figure 2). Catechol and quinone derivatives are used in cancer studies but they are susceptible to oxidation and reduction and

show low chemical stability, making them unsuitable in drug discovery.[19] Therefore, substitutions of the catechol in section B with other functional groups, such as F or OCH_3, were pursued.

The compounds with newly introduced functional groups on each aromatic ring (Figure 2, section A and B) and the cyclized compounds at 20 μM were evaluated for their potential to inhibit TNF-α production in LPS-stimulated macrophages (Figure 3). First, we assessed the activity of cyclized compound **9**, because the 2-hydroxy group at R^2 readily attacks an intramolecular Michael acceptor to generate the cyclic form, a flavanone, which could be synthesized during flavonoid biosynthesis. However, compound **9** was a weak inhibitor, so we continued to focus on functional group modifications of the open-chain structure, the chalcones. The replacement of catechol was performed to generate stable and relevant bioisosteres because catechol is susceptible to oxidation and reduction and is labile to metabolism in vivo (Figure 3). Both hydroxyl groups at the catechol in section B were substituted with OCH_3 and F (compounds **7a-e**), which resulted in the loss of TNF-α inhibition. Although the substitution of the hydroxyl group with the fluoride at R^4 generated compound **7d** (22% inhibition) with inhibitory activity similar to compound **1** (20% inhibition), compound **7d** was readily decomposed at room temperature in the presence of oxygen.

Next, the replacement of hydroxyl group R^2 was performed to enhance the chemical stability and inhibitory activity of TNF-α production as the hydroxyl group is a nucleophile and is prone to intramolecular nucleophilic attacks, which lead to the formation of a cyclized compound. Substitutions of 2-hydroxyl by 2-fluoro (**7g**, 32% inhibition) and 2-methyl (**7h**, 41% inhibition) at the R^2 on the A ring showed more efficacy for TNF-α inhibition compared

to compound **1** (20% inhibition). Also, no cyclized compounds were observed during synthesis of the desired compounds.

Compounds **7i** and **7j** replaced hydroxyl groups with alkoxy groups at C^2 and significantly suppressed TNF-α production. The more sterically hindered alkoxy group presented with greater inhibition of TNF-α production (OMe < OiPr). Compound **7j,** bearing the more sterically bulky isopropoxyl group, showed the strongest activity at 64% inhibition. However, unfortunately, **7J** decomposed at ambient temperature. Also, mono-substituted compounds **7l** (61% inhibition) with a 2-chloro and compound **7m** (62% inhibition) with a 2-methyl at R^6 showed similar efficacy to compound **7j** (64% inhibition). Furthermore, we also used a prodrug strategy to modify the physicochemical properties of compound **1** due to its low kinetic solubility (21 μg/mL) and low permeability (-5.35) in a parallel artificial membrane permeability assay (PAMPA) (Table 2, entry 1).

To design prodrugs of compound **1**, we modified the hydroxyl group at R^2 to prevent cyclization, which could occur during flavonoid biosynthesis reactions. Compounds **14a**-**d**, **8a**, and **8b** contained various acetyl and aryl esters that are typically cleaved by ubiquitous hydrolases in the plasma and during first-pass metabolism.[20,21] These compounds were also synthesized and evaluated in the TNF-α production inhibition assay at a single concentration (20 μM) (Figure 4). Compound **14a** (51% inhibition) containing a benzoyl ester at R^2 strongly reduced TNF-α production and globally acetylated compound **8a** (73% inhibition) at R^5 on the A and B rings from compound **1**, exhibited highly reproducible inhibitory activity.

To confirm the anti-inflammatory activities, we examined the dose-dependent inhibition of TNF-α production by LPS-stimulated to determine the half-maximal inhibitory concentration (IC_{50}) (Table 1). Substitution of R^2 with an electron-donating group, such as methyl or

methoxy, on the A section of the chalcone generated compounds with moderate IC_{50}. The inhibitory activity of compounds **7h** and **7i** was similar to that of compound **1** (IC_{50}, 43.3 μM). Interestingly, compounds **7l** (IC_{50}, 18.6 μM) and **7m** (IC_{50}, 17.3 μM), with the weak electron donating/withdrawing-group instead of the hydroxyl group, were two-fold more active than compound **1**. However, compound **7m** was not a suitable lead due to low solubility (28 μg/mL). Phase I metabolic stability using liver microsomes from mice, rats, and humans was evaluated by examining the percent of compound remaining 30 minutes after the compound was reacted. Compound **7m** exhibited relatively low metabolic stability in Phase I metabolism in the various species (mouse, 7%; rat, 21%; and human, 38%) (Table 2, entry 2; Table 3, entry 2). Interestingly, compound **14s** has a relatively strong inhibition of TNF-α production at a single dose (20 μM), which correlated with potency in a dose-dependent manner (Figure 4 and Table 1, entries 6-9). In a test using compounds **14b** (IC_{50}, 18.9 μM), **14c** (IC_{50}, 20.8 μM), and **14d** (IC_{50}, 17.9 μM), small donating/withdrawing groups, including methyl, methoxy, and chloro at the para-position of the benzoyl ester, exhibited two-fold more or less inhibition of LPS-induced TNF-α production than that of compound **1**, results which were similar to that of compound **14a** (IC_{50}, 14.6 μM) (Table 1, entries 6-9). Compound **8a**, which is globally acetylated at R^5 on the A and B rings, exhibited the strongest potency (IC_{50} 12.8 μM) (Table 1, entry 10). However, we decided not to test this compound in the lymphedema animal model because it was not miscible with water at high concentrations and tended to form droplets in aqueous solutions.

Importantly, we found that compounds **14a-d** were relatively strong inhibitors of TNF-α production in the single-dose test and the dose-dependency assay. We assumed that compound **1** was the pharmacologically active component for TNF-α production inhibition and investigated whether the promoiety of the prodrug could be readily cleaved by enzymatic

hydrolysis. Based on the activity profile and the physicochemical properties, we chose compound **14a** for an animal experiment using oral administration and compared its efficacy and blood concentration with those of compound **1**. The water solubility of compound **14a (**136 μg/mL) was approximately five-fold higher than that of compound **1 (**21 μg/mL) (Table 2, entry 1, 3). The blood exposure levels of the compounds during systemic circulation were compared by integrating the area under the curve (AUC) after oral administration of 100 mg/kg of compound **1** and **14a**. We found that compound **14a** was readily metabolized into compound **1** by ubiquitous hydrolytic cleavage activities in the blood plasma, even after intravenous administration. Compound **14a** was not detectable above the limit of quantitation (LOQ, < 1 ng/mL). We decided that the oral administration of compound **14a** could be estimated by monitoring compound **1** as the pharmaceutically active ingredient as it is the main metabolite derived from compound **14a**. In the pharmacokinetic study using oral administration, it was more efficient to use compound **14a** (AUC, 1224 h × ng/mL) for the delivery of compound **1** into the systemic circulation than using unmodified compound **1** (AUC, 251 h × ng/mL).

Preventive Effect of Orally Administered Compound 14a on Lymphedema Formation

Since oral administration of compound **1** decreased swelling in the murine lymphedema model, we hypothesized that the inhibitory effects of compounds **14a** and **1** may be similar, but the altered pharmacokinetic properties of compound **14a,** such as drug delivery through oral dose, could be an advantage. To test this hypothesis, we pretreated mice with compounds **1** and **14a** via oral administration for seven days before surgical induction of lymphedema. The representative dorsal images from treated mice unequivocally indicated the suppression of lymphedema swelling in the right hind limb (Figure 5A). At day seven post-surgery, the lymphedema volume was decreased by 52%, 53%, and 70% with treatment using compounds

1, **7m**, and **14a**, respectively, compared with the vehicle treated lymphedema group (Figure 5).

Histology and Molecular Analysis

We investigated H&E images from the limbs of mice in the normal group, vehicle-treated lymphedema group, and the lymphedema groups treated with compounds **1** or **14a** (Figure 6A). As a result, compound **14a** reduced neutrophil infiltration and ameliorated dermal layer lymphedematous tissue**.** TNF-α mRNA expression was assessed in the lymphedematous tissue and revealed decreased TNF-α expression with compound **1** and **14a** treatment. The group treated by compound **14a** had the lowest level of TNF-α mRNA expression, although there was no statistical difference (P-value= 0.613) in expression between the compound **1** and **14a** treatment groups. In addition, we examined the regulatory effects of compound **1** and compound **14a** on adipogenesis observed in lymphedema. The representative histologic images indicated that both compounds prevented the development of adipose tissue in the dermal layer (Figure 7A). Peroxisome proliferator-activated receptor γ (PPARγ) is the master regulator of adipogenesis. Immunofluorescence staining showed that the distribution of PPARγ protein was suppressed in the dermal layer of lymphedematous tissue following treatment with compounds **1** and **14a** (Figure 7B). Western blot analysis revealed that these compounds decreased PPARγ and its target protein, fatty acid-binding protein 4 (Fabp4) in the affected limbs (Figure 7C). Consistently, the levels of PPARγ and Fabp4 mRNA were reduced in both treatment groups, with compound **14a** being more potent than compound **1** (Figure 7D). These molecular analyses showed that compounds **1** and **14a** displayed a similar

anti-inflammatory activity but compound **14a** was more efficient in ameliorating adipogenesis during lymphedema development.

Synthesis of Compounds 7s and 14s

Compound **1** is structurally classified as a chalcone, which can be referred to as an open-chain flavonoid. Two aromatic rings are linked by a double bond and a carbonyl, which are fully conjugated. Several reports on the synthesis of chalcones have described various methods, with the most common being the base-catalyzed Claisen-Schmidt reaction in which the condensation of ketones with aldehydes is performed in the presence of an aqueous base solution.[22,23,24,25,26] However, this method has limitations leading to the decomposition of the phenol/catechol involving acidic protonation of the substrate, which affects the synthesis yield and the diversity of substances.

Syntheses of the various compounds **7s** are described in Scheme 1. The Claisen condensation of compounds **5a-j** and **6a-e** at 25 ^{o}C under basic conditions afforded compounds **1** and **7a-m** (method A)**.** Compound **1** was acylated with acetic anhydride and benzoyl chloride to produce compounds **8a** and **8b**, respectively. Because possible degradation of catechol/phenol in compounds **5b** and **5f** were observed, we alternatively performed Cu(II)-mediated catalytic aldol condensation by oxidation/reduction of Cu(II) in a tandem process to produce compounds **7h** and **7i** (method B).[27] The synthesis of 2-acylated compounds **14a-d** bearing a para-substituted benzoyl ester as a prodrug is presented in Scheme 2. The ester bond readily enables cleavage by ubiquitous hydrolases in the gastrointestinal tract and blood plasma. The selective acylation at the C2-hydroxyl group of compounds **14a-d** required global hydroxyl protection of acetophenone **10**, because the

hydroxyl group at the para-position of acetophenone **10** was predominantly reacted with acyl chlorides. Compound **5a** was reacted with methoxymethyl chloride (MOM-Cl) to generate compound **10**, which was selectively protected at the ortho hydroxyl group. Compound **11** was obtained by reacting compound **6a** with MOM-Cl. Claisen condensation of compounds **10** and **11** for 6 h in the presence of 60% KOH (aq) was carried out to produce compound **12**. Esterification of compound **12** with various acyl chloride compounds in dimethylformamide (DMF) for 3 h was followed by global MOM deprotection of compounds **13a-d** to produce the desired products (**14a-d**).

CONCLUSION

Our findings indicate that compounds having anti-inflammatory activities are potential pharmaceutical agents against the pathogenesis of acquired lymphedema. By screening natural products, we identified compound **1** as being able to suppress LPS-induced TNF-α production in inflammation. Dose-dependent inhibitory activity was confirmed in a murine peritoneal macrophage model, in vitro. For pharmaceutical properties, we modified its structure by functional group conversion to enhance the potency, solubility, and permeability. Furthermore, we designed a prodrug which could be readily converted to a pharmaceutically active ingredient by ubiquitous hydrolase in vivo activity. As a result, we determined that compound **7m** showed a three-fold higher potency (17.3 μM) for anti-inflammatory effects in vitro than compound **1** (43.3 μM). Despite its insufficient solubility (28 μg/mL), compound **7m** presented with enhanced permeability and could suppress limb swelling (53%) with oral administration (100 mg/kg/day). Compound **14a** was the most potent (14.6 μM) and had five-fold higher solubility (136 μg/mL)**.** As a prodrug, compound **14a** was immediately converted into compound **1** by the liver microsomes from three species, including mice, rats, and

humans. Compound **14a** also had the advantage of being at a higher concentration in the blood (AUC, 1224 hr × ng/mL) than compound **1** (AUC, 251 hr × ng/mL) when administered orally. Correspondingly, compound **14a** suppressed limb swelling by 70% with oral administration (100 mg/kg/day). Compound **14a** showed anti-inflammatory activity by decreasing TNF-α mRNA expression and neutrophil infiltration, and ameliorated the lymphedema in the dermal layer, as seen by H&E staining. Conclusively, the orally administered compound **14a** contributed to pharmacological suppression of inflammation and can be a potential therapy for the treatment of lymphedema.

EXPERIMENTAL SECTION

Cell Culture

For peritoneal macrophage isolation, male Balb/c mice were injected intraperitoneally with 2 mL of 3.5% sterile thioglycollate (BD, Sparks, MD, USA) four days before sacrifice. Mice were sacrificed via cervical dislocation and the peritoneal exudate cells were aseptically isolated via peritoneal lavage with cold DMEM (HyClone, Logan, UT, USA) containing 10% fetal bovine serum (FBS; HyClone) and 1% penicillin-streptomycin. After centrifugation, the cells were resuspended and counted using a TC20 Automated Cell Counter (Bio-Rad Laboratories, Hercules, CA, USA). Peritoneal exudate cells were plated in 24-well plates overnight at 37 ºC, and the non-adherent cells were removed. The cells were then stimulated with 100 ng/mL LPS for 24 h. The supernatant was collected for cytokine analysis. The levels of TNF-α in the supernatants were determined using BD OptEIA mouse ELISA sets (BD Biosciences, San Diego, CA, USA) according to the manufacturer's protocol.

Animals

All animal studies were approved by the Institutional Animal Care and Use Committee (IACUC) of Sungkyunkwan University School of Medicine (Approval Number: SKKUIACUC-20150037). All methods were conducted in accordance with the approved guidelines. The murine model for acquired lymphedema was surgically induced in the lower limb of male ICR mice, using a protocol that has been previously established.[20] Briefly, the major lymphatic components, including superficial inguinal lymph node, popliteal lymph node, deep inguinal lymph node, and a femoral lymphatic vessel were removed and limitedly cauterized in the right lower limb of mice that were under anesthesia.

Lymphedema Volume Quantitation

Lymphedema size measurements were conducted by observers blinded to the treatment status of the mice. Limb volumes were calculated on postoperative days three and seven using a caliper as previously described.[20, 21]

Histology and Immunofluorescence

Tissue samples were harvested seven days post-surgery 15–25 mm distal from the right lower limb. The collected tissues were fixed in 10% formalin solution. The specimens were cross-sectioned at a thickness of 5 μm. The sections were deparaffinized in 100% xylene, rehydrated in a graded ethanol series (100%, 95%, 90%, 80%, and 70%), and rinsed in water. Sections were stained with a hematoxylin solution at RT. After washing in PBS, sections were then stained in eosin at RT. Images were captured with a Pannoramic Viewer microscope (3DHISTECH Ltd., Hungary). Prepared slides were incubated with anti-mouse PPARγ (Santa Cruz Biotechnology, USA), Alexa Fluor 488, and DAPI (Life Technologies,

USA). Samples were analyzed under a Nikon ECLIPSE 80i microscope (Nikon Instruments Inc., Japan).

Quantitative Real-Time Polymerase Chain Reaction (RT-PCR)

Total RNA was prepared from affected tissues using TRI reagent (Invitrogen, Carlsbad, CA). Complementary DNA was synthesized from 500 ng of total RNA using M-MLV Reverse Transcriptase (Promega, USA). Quantitative RT-PCR was performed using a SYBR Mix (TOYOBO, Osaka, Japan). The gene-specific primer sets for PCR were as follows: peroxisome proliferator-activated receptor γ (Pparγ) forward, 5′-CCATTCTGGCCCACCAAC-3′ and reverse, 5′-GCACCTGCACCAGGGC-3′; CCAAT/enhancer-binding protein α (C/ebpα) forward, 5′-GCGGGCAAAGCCAAGAA-3′ and reverse, 5′-GCGTTCCCGCCGTACC-3′; Fabp4 forward, 5′-CACCGCAGACGACAGGAAG-3′ and reverse, 5′-GCACCTGCACCAGGGC-3′; CD36 forward, 5′-GGCCAAGCTATTGCGACAT-3′ and reverse, 5′-CAGATCCGAACACAGCGTAGA-3′.

Western Blot Analysis

Western blotting was performed as previously described[2]. Briefly, proteins were extracted from tissue samples using 500 μl of PRO-PREP protein extraction solution (Intron Biotechnology, Seoul, Korea). Proteins were incubated with Pparγ (1:1000, Santa Cruz Biotechnology, USA) and Fabp4 (1:1000, Santa Cruz Biotechnology, USA).

Statistical Analysis

The statistical significance of the differences between treatments was considered using an unpaired one-tailed Student's *t*-test and a one-way ANOVA, followed by the Bonferroni post-hoc test, where appropriate. All data are presented as mean ± standard deviation. P-values were presented to show the level of significance.

Pharmacokinetic Analysis of Compounds 1 and 14a

Male CD-1 mice (5 weeks) were purchased from Charles River Laboratories (Wilmington, MA). Each mouse was administered with a test compound via tail vein at 1 mg/kg or oral administration at 20 mg/kg or 100 mg/kg. Three animals were used for each independent serial sampling experiment. Blood samples were collected at 5, 15, 30, 60, 120 (or 180), 360, and 1440 min from each animal via the saphenous vein; 20-30 μL was drawn at each time point and 15 μL of blood was used for quantitative bioanalysis by HPLC-MS/MS. The fundamental pharmacokinetic parameters (half-life, clearance, volume of distribution, and AUC) were obtained from non-compartmental analysis using Win-Non-lin. This experiment performed simultaneous analysis of the analytes via the multiple reaction mirroring (MRM) mode using TQ5000 LC/MS/MS (AB/SCIEX) combined with HTC-PAL.

General Methods

All substances were purchased from Sigma-Aldrich (St. Louis, MO) and used as received. Purchased anhydrous methanol was used without further purification. Analytical thin-layer chromatography was conducted on E. Merck TLC plates (silica gel 60 F_{254}, aluminum back).

Silica gel 60 (230–400 mesh) for column chromatography was purchased from E. Merck. Melting points were measured with a Kofler block or a Büchi melting point apparatus, model B-545. The ^{1}H and ^{13}C NMR spectroscopic data were recorded in $CDCl_3$, DMSO-d_6, and CD_3OD solutions at ambient temperature with Avance II 400 (Bruker BioSpin, Germany) (400 MHz for ^{1}H NMR and 100 MHz for ^{13}C NMR) and Ascend III 700 (Bruker BioSpin, Germany) (700 MHz for ^{1}H NMR and 175 MHz for ^{13}C NMR). Chemical shifts were recorded as δ values in parts per million (ppm) and were indirectly referenced to tetramethylsilane by the solvent signal. Coupling constants (*J*) were reported in Hertz. Infrared spectra were recorded on a Nicolet 6700 FTIR spectrophotometer. Low-resolution mass spectra were measured on a Micromass Quattro Micro API (Waters, USA), whereas high-resolution mass spectra were recorded on an LTQ Orbitrap XL (Thermo Scientific, USA) spectrometer. Characterization data for known compounds were consistent with literature values.

Representative Compounds and Their Synthetic Procedures

All compounds were synthesized as shown in Scheme 1 (compounds **1**, **7a-m**, **8a-b**, and **9**) or Scheme 2 (compounds **14a-d**), except the commercially available compounds (compounds **2**, **3**).

General Procedure for Butein Derivatives

Method A

Syntheses of *(E)*-1-(2, 4-dihydroxyphenyl)-3-phenylprop-2-en-1-one (1)

3,4-Dihydroxybenzaldehyde **6a** (1.0 g, 7.2 mmol) and 1-(2,4-dihydroxyphenyl)ethan-1-one **5a** (1.1 g, 7.2 mmol) were dissolved in ethanol (10 mL). An aqueous solution of 60% KOH (1 mL) was added and the mixture was incubated at room temperature for 6 h. Solvents were removed under reduced pressure and the residue was extracted three times with 30 mL of diethyl ether. The diethyl ether layer was washed three times with 30 mL of water and dried over anhydrous $MgSO_4$. After solvent removal, the product was purified by silica gel column chromatography (silica gel, n-hexane-ethyl acetate, 1:1) to produce the indicated product. *(E)*-1-(2,4-dihydroxyphenyl)-3-(3,4-dihydroxyphenyl)prop-2-en-1-one (**1**) as a yellow solid (42%); ^{1}H NMR (MeOD, 400 MHz) δ 7.95 (1H, d, *J* = 8.8 Hz), 7.73 (1H, d, *J* = 15.6 Hz), 7.54 (1H, d, *J* = 15.6 Hz), 7.20 (1H, d, *J* = 2.0 Hz), 7.12 (1H, dd, *J* = 8.4, 2.4 Hz), 6.83 (1H, d, *J* = 8.4 Hz), 6.43 (1H, dd, *J* = 8.8, 2.4 Hz), 6.31 (1H, d, *J* = 2.4 Hz; ^{13}C NMR (100 MHz, MeOD) δ 193.50, 167.52, 166.37, 149.95, 146.86, 146.11, 133.30, 128.45, 123.64, 118.31, 116.63, 115.84, 114.74, 109.17, 103.85; LRMS (ESI) calcd. for $C_{15}H_{13}O_5$ $[M+H]^+$: 273.08 found : 273.10; HRMS (ESI) calcd. for $C_{15}H_{13}O_5$ $[M+H]^+$: 273.0685, found : 273.0754; m.p. = 214.7 °C.

Method B

1-(4-Hydroxy-2-methylphenyl)ethan-1-one **5b** (150 mg, 1.0 mmol), 2,4-dihydroxybenzaldehyde **6a** (138 mg, 1.0 mmol), and $CuBr_2$ (22 mg, 0.1 mmol) in a pressured tube were dissolved in 5 mL ethyl acetate at room temperature. The reaction mixture was stirred at 80 °C. After 12 h the mixture was cooled to room temperature and filtered through Celite. The organic layer was concentrated in *vacuo* and the product, **7h** (66%), was a yellow solid that was purified by silica gel column chromatography (silica gel, n-hexane-ethyl acetate, 1:1).

***(E)*-1-(2,4-Dihydroxyphenyl)-3-(4-hydroxy-3-methoxyphenyl)prop-2-en-1-one (7a)**

The title compound via method A was isolated as a yellow solid (46%); ^{1}H NMR (MeOD, 400 MHz) δ 7.93 (1H, d, *J* = 8.8 Hz), 7.69 (1H, d, *J* = 15.2 Hz), 7.55 (1H, d, *J* = 15.2 Hz), 7.27 (1H, d, *J* = 2.0 Hz), 7.12 (1H, dd, *J* = 8.4, 2.0 Hz), 6.75 (1H, d, *J* = 8.0 Hz), 6.31 (1H, dd, *J* = 8.8, 2.4 Hz), 6.19 (1H, d, *J* = 2.4 Hz) 3.84 (3H, s); ^{13}C NMR (100 MHz, MeOD) δ 193.4, 167.5, 166.4, 151.7, 148.0, 145.5, 133.4, 129.5, 123.5, 119.2, 115.2, 114.7, 112.5, 109.2, 103.8, 56.56; LRMS (ESI) calcd. for $C_{16}H_{15}O_5$ $[M+H]^+$: 287.09, found : 287.10; HRMS (ESI) calcd. for $C_{16}H_{15}O_5$ $[M+H]^+$: 287.0914, found : 287.0908; m.p. = 198.1 °C.

***(E)*-1-(2,4-Dihydroxyphenyl)-3-(3-hydroxy-4-methoxyphenyl)prop-2-en-1-one (7b)**

The title compound via method A was isolated as a yellow solid (48%); ^{1}H NMR (400 MHz, MeOD) δ 7.96 (1H, d, *J* = 8.0 Hz), 7.74 (1H, d, *J* = 15.6 Hz), 7.59 (1H, d, *J* = 15.2 Hz), 7.25 (1H, d, *J* = 2.4 Hz), 7.20 (1H, dd, *J* = 8.4, 2.0 Hz), 6.98 (1H, d, *J* = 8.4 Hz), 6.43 (1H, dd, *J* = 8.8, 2.4 Hz), 6.31 (1H, d, *J* = 2.4 Hz) 3.92 (3H, s); ^{13}C NMR (100 MHz, MeOD) δ 193.4, 167.5, 166.4, 151.7, 148.0, 145.5, 133.4, 129.5, 123.5, 119.2, 115.2, 114.7, 112.5, 109.2, 103.8, 56.39; LRMS (ESI) calcd. for $C_{16}H_{15}O_5$ $[M+H]^+$: 287.09, found : 287.10; HRMS (ESI) calcd. for $C_{16}H_{15}O_5$ $[M+H]^+$: 287.0914, found : 287.0908; m.p. = 206.4 °C.

***(E)*-1-(2,4-Dihydroxyphenyl)-3-(3-fluoro-4-hydroxyphenyl)prop-2-en-1-one (7c)**

The title compound via method A was isolated as a yellow solid (53%); ^{1}H NMR (400 MHz, MeOD δ 7.99 (1H, d, *J* = 8.8 Hz), 7.75 (1H, d, *J* = 15.2 Hz), 7.65 (1H, d, *J* = 15.6 Hz), 7.57 (1H, dd, *J* = 12.4, 2.0 Hz), 7.39 (1H, dd, *J* = 8.4, 1.6 Hz), 6.97 (1H, t, *J* = 8.8 Hz), 6.43 (1H, dd, *J* = 8.8, 2.4 Hz), 6.30 (1H, d, *J* = 2.4 Hz); ^{13}C NMR (100 MHz, MeOD) δ 193.2, 167.5, 166.5, 154.2, 151.9, 149.1, 144.1, 133.5, 127.4, 119.9, 118.9, 116.5, 114.6, 109.2, 103.8;

LRMS (ESI) calcd. for $C_{15}H_{12}O_4F$ $[M+H]^+$: 275.07, found : 275.10; HRMS (ESI) calcd. for $C_{15}H_{12}O_4F$ $[M+H]^+$: 275.0714, found : 275.0709; m.p. = 210.5 °C.

***(E)*-1-(2,4-Dihydroxyphenyl)-3-(4-fluoro-3-hydroxyphenyl)prop-2-en-1-one (7d)**

The title compound via method A was isolated as a yellow solid (52%); ^{1}H NMR (400 MHz, MeOD) δ 7.98 (1H, d, *J* = 8.8 Hz), 7.74 (1H, d, *J* = 15.6 Hz), 7.67 (1H, d, *J* = 15.6 Hz), 7.32 (1H, dd, *J* = 8.4, 2.0 Hz), 7.25 - 7.21 (1H, m), 7.15 - 7.10 (1H, m), 6.44 (1H, dd, *J* = 8.8, 2.4 Hz), 6.31 (1H, d, *J* = 2.4 Hz); ^{13}C NMR (100 MHz, MeOD) δ 193.2, 167.6, 166.7, 155.7, 146.7, 144.3, 133.5, 133.2, 122.0, 121.4, 118.5, 117.4, 114.6, 109.3, 103.8; LRMS (ESI) calcd. for $C_{15}H_{12}O_4F$ $[M+H]^+$: 275.07, found : 275.10; HRMS (ESI) calcd. for $C_{15}H_{12}O_4F$ $[M+H]^+$: 275.0714, found : 275.0709; m.p. = 252.4 °C.

(E)-1-(2,4-Dihydroxyphenyl)-3-(4-hydroxyphenyl)prop-2-en-1-one (7e)

The title compound via method A was isolated as a yellow solid (43%); ^{1}H NMR (400 MHz, MeOD) δ 7.98 (1H, d, *J* = 9.2 Hz), 7.80 (1H, d, *J* = 15.2 Hz), 7.64 - 7.60 (3H, m), 6.86 (2H, d, *J* = 8.0 Hz), 6.43 (1H, dd, *J* = 8.8, 2.4 Hz), 6.31 (1H, d, *J* = 2.4 Hz); ^{13}C NMR (100 MHz, MeOD) δ 193.5, 167.5, 166.3, 161.5, 145.6, 133.3, 131.8, 127.8, 118.5, 116.9, 114.7, 109.1, 103.8; LRMS (ESI) calcd. for $C_{15}H_{13}O_4$ $[M+H]^+$: 257.08, found : 257.10; HRMS (ESI) calcd. for $C_{15}H_{13}O_4$ $[M+H]^+$: 257.0801, found : 257.0801; m.p. = 205.7 °C.

***(E)*-1-(2,4-Dihydroxyphenyl)-3-(3-hydroxyphenyl)prop-2-en-1-one (7f)**

The title compound via method A was isolated as a yellow solid (52%); ^{1}H NMR (400 MHz, MeOD) δ 8.00 (2H, d, *J* = 8.8 Hz), 7.66 (1H, d, *J* = 15.6 Hz), 7.51 (1H, d, *J* = 15.2 Hz), 7.19

(1H, d, *J* = 2.4 Hz), 7.11 (1H, dd, *J* = 8.0, 2.0 Hz), 6.91 (2H, d, *J* = 8.8 Hz), 6.83 (1H, d, *J* = 8.0 Hz); ^{13}C NMR (100 MHz, MeOD) δ 191.0, 163.7, 149.8, 146.2, 132.2, 131.2, 128.4, 123.4, 119.5, 116.6, 116.4, 115.6; LRMS (ESI) calcd. for $C_{15}H_{13}O_4$ $[M+H]^+$: 257.08, found : 257.10; HRMS (ESI) calcd. for $C_{15}H_{13}O_4$ $[M+H]^+$: 257.0808, found : 257.0803; m.p. = 208.0 °C.

***(E)*-3-(3,4-Dihydroxyphenyl)-1-(2-fluoro-4-hydroxyphenyl)prop-2-en-1-one (7g)**

The title compound via method A was isolated as a yellow solid (53%); ^{1}H NMR (400 MHz, MeOD) δ 7.75 (1H, t, *J* = 8.8 Hz), 7.62 (1H, dd, *J* = 15.6, 2.0 Hz), 7.28 (1H, dd, *J* = 15.2, 2.4 Hz), 7.14 (1H, d, *J* = 2.0 Hz), 7.19 (1H, d, *J* = 2.4 Hz), 7.04 (1H, dd, *J* = 8.4, 2.0 Hz), 6.82 (1H, d, *J* = 8.0 Hz), 6.72 (1H, dd, *J* = 8.8, 2.4 Hz), 6.61 (1H, dd, *J* = 13.2, 2.4 Hz); ^{13}C NMR (100 MHz, MeOD) δ 189.5, 165.0, 150.0, 146.8, 133.6, 128.2, 123.6, 123.2, 119.6, 116.6, 115.4, 113.1, 104.2, 103.9; LRMS (ESI) calcd. for $C_{15}H_{12}O_4F$ $[M+H]^+$: 275.08, found : 275.10; HRMS (ESI) calcd. for $C_{15}H_{12}O_4F$ $[M+H]^+$: 275.0714, found : 275.0708; m.p. = 207.8 °C.

***(E)*-3-(3,4-Dihydroxyphenyl)-1-(4-hydroxy-2-methylphenyl)prop-2-en-1-one (7h)**

The title compound via method B was isolated as a yellow solid (66%); ^{1}H NMR (400 MHz, MeOD) δ 7.54 (1H, d, *J* = 9.2 Hz), 7.41 (1H, d, *J* = 15.6 Hz), 7.12 (1H, d, *J* = 2.4 Hz), 7.09 (1H, d, *J* = 16.0 Hz), 7.02 (1H, dd, *J* = 8.0, 2.0 Hz), 6.81 (1H, d, *J* = 8.4 Hz), 6.73 - 6.70 (2H, m), 2.42 (3H, s); ^{13}C NMR (100 MHz, MeOD) δ 197.0, 161.3, 149.9, 147.3, 146.8, 141.7, 132.5, 131.6, 128.1, 124.0, 123.4, 119.2, 116.5, 115.4, 113.3, 21.26; LRMS (ESI) calcd. for

$C_{16}H_{15}O_4$ $[M+H]^+$: 271.10, found : 271.10; HRMS (ESI) calcd. for $C_{16}H_{15}O_4$ $[M+H]^+$: 271.0965, found : 271.0958; m.p. = 208.2 °C.

***(E)*-3-(3,4-Dihydroxyphenyl)-1-(4-hydroxy-2-methoxyphenyl)prop-2-en-1-one (7i)**

The title compound via method B was isolated as a yellow solid (46%); ^{1}H NMR (400 MHz, MeOD) δ 7.59 (1H, d, *J* = 8.8 Hz), 7.51 (1H, d, *J* = 15.6 Hz), 7.38 (1H, d, *J* = 15.2 Hz), 7.12 (1H, d, *J* = 2.0 Hz), 7.00 (1H, dd, *J* = 8.4, 2.0 Hz), 6.80 (1H, d, *J* = 8.0 Hz), 6.53 (1H, d, *J* = 2.0 Hz), 6.47 (1H, dd, *J* = 8.4, 2.0 Hz), 3.91 (3H, s); ^{13}C NMR (100 MHz, MeOD) δ 193.0, 164.5, 162.5, 149.5, 146.8, 144.5, 133.7, 128.6, 125.1, 123.3, 121.7, 116.5, 115.2, 108.9, 100.1, 56.15; LRMS (ESI) calcd. for $C_{16}H_{15}O_5$ $[M+H]^+$: 287.09, found : 287.10; HRMS (ESI) calcd. for $C_{16}H_{15}O_5$ $[M+H]^+$: 287.0914, found : 287.0906; m.p. = 200.4 °C.

***(E)*-3-(3,4-Dihydroxyphenyl)-1-(4-hydroxy-2-isopropoxyphenyl)prop-2-en-1-one (7j)**

The title compound via method A was isolated as a yellow solid (53%); ^{1}H NMR (400 MHz, MeOD) δ 7.58 (1H, d, *J* = 8.8 Hz), 7.47 (2H, d, *J* = 2.8 Hz), 7.11 (1H, d, *J* = 2.0 Hz), 7.00 (1H, dd, *J* = 8.4, 2.4 Hz), 6.81 (1H, d, *J* = 8.0 Hz), 6.51 (1H, d, *J* = 2.4 Hz), 6.45 (1H, dd, *J* = 8.8, 2.4 Hz), 4.69 (1H, hept, 6.0 Hz), 1.40 (6H, d, *J* = 6.0 Hz); ^{13}C NMR (100 MHz, MeOD) δ 193.4, 160.6, 146.8, 143.9, 133.7, 128.7, 125.5, 123.1, 122.9, 116.5, 115.2, 109.1, 102.2, 72.21, 22.43; LRMS (ESI) calcd. for $C_{18}H_{19}O_5$ $[M+H]^+$: 315.12, found : 315.20; HRMS (ESI) calcd. for $C_{18}H_{19}O_5$ $[M+H]^+$: 315.1227, found : 315.1219; m.p. = 80.4 °C.

***(E)*-3-(3,4-Dihydroxyphenyl)-1-(2,4-dimethoxyphenyl)prop-2-en-1-one (7k)**

The title compound via method A was isolated as a yellow solid (63%); ^{1}H NMR (400 MHz, MeOD) δ 7.65 (1H, d, *J* = 8.4 Hz), 7.51 (1H, d, *J* = 15.6 Hz), 7.34 (1H, d, *J* = 15.6 Hz), 7.12 (1H, d, *J* = 2.0 Hz), 7.00 (1H, dd, *J* = 8.4, 2.0 Hz), 6.81 (1H, d, *J* = 8.4 Hz), 6.65 - 6.61 (2H, m), 3.93 (3H, s), 3.89 (3H, s); ^{13}C NMR (100 MHz, MeOD) δ 193.3, 166.0, 162.0, 149.7, 146.8, 145.0, 133.4, 128.5, 124.9, 123.4, 116.5, 115.2, 106.7, 99.53, 56.20; LRMS (ESI) calcd. for $C_{17}H_{17}O_5$ $[M+H]^+$: 301.10, found : 301.10; HRMS (ESI) calcd. for $C_{17}H_{17}O_5$ $[M+H]^+$: 301.1071, found : 301.1065; m.p. = 162.9 °C.

(*E*)-3-(3,4-Dihydroxyphenyl)-1-(p-tolyl)prop-2-en-1-one (7l)

The title compound via method A was isolated as a yellow solid (66%); ^{1}H NMR (400 MHz, MeOD) δ 7.96 (2H, d, *J* = 8.0 Hz), 7.68 (1H, d, *J* = 15.6 Hz), 7.50 (1H, d, *J* = 15.2 Hz), 7.36 (2H, d, *J* = 8.0 Hz), 7.20 (1H, d, *J* = 2.0 Hz), 7.11 (1H, dd, *J* = 8.4, 2.4 Hz), 6.83 (1H, d, *J* = 8.4 Hz), 2.44 (3H, s); ^{13}C NMR (100 MHz, MeOD) δ 192.2, 150.0, 147.0, 146.8, 145.0, 137.1, 130.4, 129.6, 128.3, 123.6, 119.6, 116.6, 115.7, 21.64; LRMS (ESI) calcd. for $C_{16}H_{15}O_3$ $[M+H]^+$: 255.10, found : 255.10; HRMS (ESI) calcd. for $C_{16}H_{15}O_3$ $[M+H]^+$: 255.1016, found : 255.1014; m.p. = 190.9 °C.

***(E)*-1-(4-Chlorophenyl)-3-(3,4-dihydroxyphenyl)prop-2-en-1-one (7m)**

The title compound via method A was isolated as a yellow solid (63%); ^{1}H NMR (400 MHz, MeOD) δ 8.06 (2H, d, *J* = 8.8 Hz), 7.71 (1H, d, *J* = 15.6 Hz), 7.56 (2H, d, *J* = 8.8 Hz), 7.49 (1H, d, *J* = 15.6 Hz), 7.21 (1H, d, *J* = 2.0 Hz), 7.14 (1H, dd, *J* = 8.4, 2.4 Hz), 6.84 (1H, d, *J* = 8.4 Hz); ^{13}C NMR (100 MHz, MeOD) δ 191.1, 147.8, 146.9, 140.0, 138.2, 131.1, 129.9, 128.1, 123.8, 119.1, 116.6, 115.8; LRMS (ESI) calcd. for $C_{15}H_{12}O_3Cl$ $[M+H]^+$: 275.05, found

: 275.10; HRMS (ESI) calcd. for $C_{15}H_{12}O_3Cl$ $[M+H]^+$: 275.0469, found : 275.0465; m.p. = 205.4 °C.

Syntheses of *(E)*-4-(3-(2,4-diacetoxyphenyl)-3-oxoprop-1-en-1-yl)-1,2-phenylene diacetate (8a)

A solution of *(E)*-1-(2,4-dihydroxyphenyl)-3-(3,4-dihydroxyphenyl)prop-2-en-1-one **1** (500 mg, 1.8 mmol) in Ac_2O (8 mL) was heated to 120-130 °C and stirred for 5 h at this temperature. After cooling to r.t., the resulting mixture was concentrated in *vacuo*. The residue was purified by column chromatography (silica gel, n-hexane-ethylacetate, 1:2) afforded compound. *(E)*-4-(3-(2,4-Diacetoxyphenyl)-3-oxoprop-1-en-1-yl)-1,2-phenylene diacetate (**8a**) as a white solid (397 mg, 90%); ^{1}H NMR (400 MHz, MeOD) δ 7.86 (2H, d, *J* = 8.4 Hz), 7.63 - 7.61 (2H, m), 7.58 (1H, d, *J* = 16.0 Hz), 7.35 (1H, d, *J* = 12.4 Hz), 7.31 (1H, d, *J* = 5.2 Hz), 7.22 (1H, dd, *J* = 8.4, 2.4 Hz), 7.10 (1H, d, *J* = 2.4 Hz), 2.33 (3H, s), 2.31 (6H, d, *J* = 3.2 Hz), 2.23 (3H, s); ^{13}C NMR (100 MHz, MeOD) δ 188.8, 168.6, 168.0, 153.4, 149.5, 143.7, 142.4, 142.3, 133.1, 131.2, 128.9, 127.5, 125.4, 124.1, 123.3, 119.6, 117.6, 20.76, 20.32; LRMS (ESI) calcd. for $C_{23}H_{21}O_9$ $[M+H]^+$: 441.12, found : 441.10; HRMS (ESI) calcd. for $C_{23}H_{21}O_9$ $[M+H]^+$: 441.1180, found : 441.1171; m.p. = 131.3 °C.

Syntheses of *(E)*-4-(3-(2,4-bis(benzoyloxy)phenyl)-3-oxoprop-1-en-1-yl)-1,2-phenylene dibenzoate (8b)

(E)-1-(2,4-Dihydroxyphenyl)-3-(3,4-dihydroxyphenyl)prop-2-en-1-one **1** (500 mg, 1.8 mmol) was dissolved in anhydrous pyridine (5 mL), treated with benzoylchloride (2.1 ml, 18.4 mmol), refluxed for 4 h, left overnight at 22-24 °C, and diluted on the following day with

cold H_2O. The residue was extracted three times with ethyl acetate 30 ml. The ethyl acetate layer was washed three times with water (30 ml x 3) and dried over anhydrous $MgSO_4$. After removal of the solvents, the product was purified by silica gel column chromatography (silica gel, n-hexane-ethylacetate, 1:2) as the eluent to give the indicated product. *(E)*-4-(3-(2,4-bis(benzoyloxy)phenyl)-3-oxoprop-1-en-1-yl)-1,2-phenylene dibenzoate (**8b**) as a white solid (413 mg, 60%); ^{1}H NMR (400 MHz, MeOD) δ 8.24 - 8.21 (2H, m), 8.16 - 8.13 (2H, m), 8.05 - 7.99 (6H, m), 7.65 - 7.57 (7H, m), 7.51 - 7.37 (11H, m); ^{13}C NMR (100 MHz, MeOD) δ 188.6, 164.2, 163.4, 153.7, 149.7, 143.7, 142.4, 134.2, 133.4, 132.7, 131.1, 129.7, 129.6, 129.4, 129.2, 128.9, 128.4, 128.1, 127.8, 125.7, 124.1, 123.2, 120.1, 118.0; LRMS (ESI) calcd. for $C_{43}H_{29}O_9$ $[M+H]^+$: 689.18, found : 689.20; HRMS (ESI) calcd. for $C_{43}H_{29}O_9$ $[M+H]^+$: 689.1812, found : 689.1794; m.p. = 36.7 °C.

Syntheses of 1-(2-hydroxy-4-(methoxymethoxy)phenyl)ethanone (10)

1-(2,4-Dihydroxyphenyl)ethanone **5a** (1.5 g, 10 mmol) in 12 mL acetone was added K_2CO_3 (1.4 g, 10 mmol) followed by slow addition of chloro(methoxy)methane (885 mg, 11 mmol) with stirring under Ar atmosphere at rt. The reaction mixture was stirred at r.t for 4 h and filtered. Solid was washed with EtOAc (80 mL) and the combined filtrate was washed with NaH_2PO_4 (sat. 50 mL) and water (80 mL) and dried over $MgSO_4$ and concentrated. The crude product was purified with silica chromatography (n-hexane-ethylacetate, 1:4) to afford 1-(2-hydroxy-4-(methoxymethoxy)phenyl)-ethanone **10** as a off-white solid (1.2 g, 61%); ^{1}H NMR (400 MHz, DMSO-d_6) δ 12.49 (1H, s), 7.85 (1H, d, J = 8.8 Hz) 6.60 (1H, dd, J = 8.8, 2.4 Hz), 5.53 (1H, d, J = 2.4 Hz), 5.27 (2H, s), 3.39 (3H, s), 2.57 (3H, s); ^{13}C NMR (100 MHz, DMSO-d_6) δ 203.1, 163.5, 133.2, 114.5, 108.0, 102.9, 93.62, 55.90, 26.71; HRMS

(ESI) calcd. for $C_{10}H_{12}O_4$ $[M+H]^+$: 197.08, found : 197.10; HRMS (ESI) calcd. for $C_{10}H_{12}O_4$ $[M+H]^+$: 197.0825, found : 197.0815; m.p. = 60.2 °C.

Syntheses of 3,4-bis(methoxymethoxy)benzaldehyde (11)

Potassium carbonate (4.0 g, 19 mmol) and methoxymethyl chloride (2.3 g, 2.2 mL, 19 mmol) were added to a solution of 3,4-dihydroxybenzaldehyde **6a** (1 g, 7.2 mmol) in acetone (40 mL). The mixture was refluxed for 2.5 h. The precipitate was filtered and dispatched. The solvent was removed under reduced pressure. The residue was dissolved in CH_2Cl_2 (30 mL), washed with water (80 mL) and dried over $MgSO_4$ and concentrated. The crude product was purified with silica chromatography (n-hexane-ethylacetate, 1:4) to afford 3,4-bis(methoxymethoxy)benzaldehyde (**11**) as white solid (1.1 g, 70 %); ^{1}H NMR (400 MHz, DMSO-d_6) δ 9.85 (1H, s), 7.60 - 7.58 (2H, m), 7.31 (1H, d, J = 8.0 Hz), 5.30 (4H, d, J = 23.6 Hz), 3.42 (6H, d, J = 2.0 Hz); ^{13}C NMR (100 MHz, DMSO-d_6) δ 191.3, 152.1, 146.9, 130.5, 126.1, 115.6, 115.3, 94.67, 94.34, 55.97, 55.79; HRMS (ESI) calcd. for $C_{11}H_{14}O_5$ $[M+H]^+$: 227.09, found : 227.10; HRMS (ESI) calcd. for $C_{11}H_{14}O_5$ $[M+H]^+$: 227.0935, found : 227.0935; m.p. = 44.6 °C.

Syntheses of *(E)*-3-(3,4-bis(methoxymethoxy)phenyl)-1-(2-hydroxy-4-(methoxymethoxy) -phenyl)-prop-2-en-1-one (12)

1-(2-Hydroxy-4-(methoxymethoxy)phenyl)-ethanone **10** (1.0 g, 5.09 mmol) and 3,4-bis(methoxymethoxy)benzaldehyde **11** (1.2 g, 5.09 mmol) were dissolved in ethanol (10 mL). 60% KOH (aq) (2 mL) was added, and the mixture was at r.t for 6 h. Solvents were removed

under reduced pressure, and the residue was extracted three times with diethyl ether 30 ml. The diethyl ether layer was washed three times with water (30 ml x 3) and dried over anhydrous $MgSO_4$. After removal of the solvents, the product was purified by silica gel column chromatography (silica gel, n-hexane-ethylacetate, 1:2) as the eluent to give the indicated product. *(E)*-3-(3,4-Bis(methoxymethoxy)phenyl)-1-(2-hydroxy-4-(methoxymeth-

oxy)phenyl)-prop-2-en-1-one (**12**) as a yellow solid (1.3 g, 63%); ^{1}H NMR (700 MHz, DMSO-d_6) δ 13.36 (1H, s), 8.25 (1H, dd, *J* = 9.1, 3.5 Hz), 7.88 (1H, dd, *J* = 15.4, 3.5 Hz), 7.77 (1H, dd, *J* = 15.4, 3.5 Hz), 7.76 - 7.68 (1H, m), 7.52 - 7.50 (1H, m), 7.18 (1H, dd, *J* = 8.4, 4.2 Hz), 6.66 - 6.64 (1H, m), 6.59 - 6.58 (1H, m) 5.29 (3H, dd, *J* = 13.3, 4.2 Hz) 3.45 (3H, d, *J* = 4.2 Hz), 3.41 (6H, dd, *J* = 7.7, 4.2 Hz); ^{13}C NMR (175 MHz, DMSO-d_6) δ 133.0, 129.2, 125.2, 120.1, 117.7, 117.0, 115.2, 108.6, 103.6, 95.53, 95.12, 94.33, 56.51, 56.43, 56.37; HRMS (ESI) calcd. for $C_{21}H_{24}O_8$ $[M+H]^+$: 405.16, found : 405.10; HRMS (ESI) calcd. for $C_{21}H_{24}O_8$ $[M+H]^+$: 405.1582, found : 405.1592; m.p. = 107.8 °C.

Syntheses of *(E)*-2-(3-(3,4-bis(methoxymethoxy)phenyl)acryloyl)-5-(methoxymethoxy) phenyl benzoate (13a)

(E)-3-(3,4-Bis(methoxymethoxy)phenyl)-1-(2-hydroxy-4-(methoxymethoxy)phenyl)prop-2-en-1-one **12** (500mg, 1.0 mmol) was dissolved in methylene chloride (10 mL). TEA (164 μL, 1.18 mmol) and benzoylchloride (137 μL, 1.18 mmol) were added, and the mixture was at r.t for 6 h. Solvents were removed under reduced pressure, and the residue was extracted three times with ethyl acetate 20 ml. The ethyl acetate layer was washed three times with water (20 ml x 3) and dried over anhydrous $MgSO_4$. After removal of the solvents, the product was purified by silica gel column chromatography (silica gel, n-hexane-ethylacetate, 1:2) as the

eluent to give the indicated product. *(E)*-2-(3-(3,4-Bis(methoxymethoxy)phenyl)acrylo-yl)-5-(methoxymethoxy)-phenyl benzoate (**13a**) as a yellow solid (430 mg, 86%); ^{1}H NMR (700 MHz, DMSO-d_6) δ 7.97 (2H, d, *J* = 7.7 Hz), 7.92 (1H, d, *J* = 9.1 Hz), 7.43 (1H, d, *J* = 11.9 Hz), 7.35 (1H, d, *J* = 14.7 Hz), 7.32 (1H, d, *J* = 7.7 Hz), 7.25 (1H, d, *J* = 8.4 Hz), 7.12 (1H, d, *J* = 8.4 Hz), 7.08 (2H, d, *J* = 9.1 Hz), 5.33 (2H, s), 5.23 (4H, d, *J* = 19.6 Hz), 3.42 (9H, t, *J* = 8.1 Hz), 2.38 (3H, s) ^{13}C NMR (175 MHz, DMSO-d_6) δ 188.8, 164.8, 160.7, 150.9, 149.8, 147.2, 144.8, 143.8, 132.1, 130.3, 129.7, 129.5, 129.0, 126.4, 126.1, 124.4, 124.0, 117.2, 116.9, 114.1, 111.7, 95.49, 95.12, 94.52, 56.43, 56.36, 56.32, 21.63; HRMS (ESI) calcd. for $C_{29}H_{30}O_9$ $[M+H]^+$: 523.20, found : 523.20; HRMS (ESI) calcd. for $C_{29}H_{30}O_9$ $[M+H]^+$: 523.2006, found : 523.2006; m.p. = 47.2 °C.

Syntheses of *(E)*-2-(3-(3,4-dihydroxyphenyl)acryloyl)-5-hydroxyphenyl benzoate (14a)

(E)-2-(3-(3,4-Bis(methoxymethoxy)phenyl)acryloyl)-5-(methoxymethoxy)phenyl benzoate **13a** (400 mg, 0.787 mmol) was dissolved in methanol (1.5 mL) and 0.25 mL of concentrated hydrochloric acid were added. The mixture was heated to 45 ^{o}C for 2 h. Evaporation of the solvent under reduced pressure provided a solid residue, which was dissolved in ethylacetate (10 mL) and washed with a $NaHCO_3$-saturated solution (3 × 20 mL). The organic phase was dried over $MgSO_4$. After removal of the solvents, the product was purified by silica gel column chromatography (silica gel, n-hexane-ethylacetate, 1:1) as the eluent to give the indicated product. *(E)*-2-(3-(3,4-Dihydroxyphenyl)acryloyl)-5-hydroxyphenyl benzoate (**14a**) as a yellow solid (220 mg, 74%); ^{1}H NMR (400 MHz, MeOD) δ 8.12 (2H, dd, *J* = 8.4, 1.6 Hz), 7.75 (1H, d, *J* = 8.4 Hz), 7.65 - 7.60 (1H, m), 7.47 (2H, t, *J* = 8.4 Hz), 7.42 (1H, d, *J* = 15.6 Hz), 7.11 (1H, d, *J* = 16.0 Hz), 6.89 - 6.85 (2H, m), 6.73 - 6.70 (2H, m); ^{13}C NMR (100 MHz, MeOD) δ 192.1, 166.5, 152.5, 149.8, 146.7, 134.9, 133.1, 131.2, 130.4, 129.7, 1.9,

125.2, 123.4, 123.0, 116.4, 115.5, 114.3, 111.4; LRMS (ESI) calcd. for $C_{22}H_{17}O_6$ $[M+H]^+$: 377.10, found : 377.10; HRMS (ESI) calcd. for $C_{22}H_{17}O_6$ $[M+H]^+$: 377.1020, found : 377.1007; m.p. = 204.9 °C.

***(E)*-2-(3-(3,4-Dihydroxyphenyl)acryloyl)-5-hydroxyphenyl 4-methylbenzoate (14b)**

The title compound was isolated as a yellow solid (51%); ^{1}H NMR (400 MHz, MeOD) δ 7.98 (2H, d, *J* = 8.0 Hz), 7.74 (1H, d, *J* = 15.6 Hz), 7.39 (1H, d, *J* = 8.4 Hz), 7.26 (2H, d, *J* = 7.6 Hz), 7.08 (1H, d, *J* = 16.0 Hz), 6.92 (1H, d, *J* = 2.0 Hz), 6.86 - 6.82 (2H, m), 6.71 - 6.68 (2H, m), 2.40 (3H, s); ^{13}C NMR (100 MHz, MeOD) δ 192.1, 166.6, 163.5, 152.6, 149.8, 146.6, 146.1, 133.1, 131.2, 130.3, 128.0, 127.5, 125.3, 123.4, 123.2, 116.3, 115.4, 114.3, 111.4, 21.72; LRMS (ESI) calcd. for $C_{23}H_{19}O_6$ $[M+H]^+$: 391.12, found : 391.10; HRMS (ESI) calcd. for $C_{23}H_{19}O_6$ $[M+H]^+$: 391.1176, found : 391.1171; m.p. = 185.7 °C.

(*E*)-2-(3-(3,4-dihydroxyphenyl)acryloyl)-5-hydroxyphenyl 4-methoxybenzoate (14c)

The title compound was isolated as a brown solid (44%); ^{1}H NMR (400 MHz, MeOD) δ 8.05 (2H, d, *J* = 8.8 Hz), 7.73 (1H, d, *J* = 8.4 Hz), 7.39 (1H, d, *J* = 15.6 Hz), 7.09 (1H, d, *J* = 15.6 Hz), 6.95 - 6.93 (3H, m), 6.86 - 6.82 (2H, m), 6.71 - 6.69 (2H, m), 3.85 (3H, s); ^{13}C NMR (100 MHz, MeOD) δ 192.1, 166.2, 165.7, 163.5, 152.7, 149.8, 146.6, 146.4, 133.4, 133.1, 128.0, 125.5, 123.4, 123.3, 122.3, 116.3, 115.4, 115.0, 114.3, 111.4, 56.07; LRMS (ESI) calcd. for $C_{23}H_{19}O_7$ $[M+H]^+$: 407.11, found : 407.10; HRMS (ESI) calcd. for $C_{23}H_{19}O_7$ $[M+H]^+$: 407.1125, found : 407.1116; m.p. = 161.1 °C.

***(E)*-2-(3-(3,4-Dihydroxyphenyl)acryloyl)-5-hydroxyphenyl 4-chlorobenzoate (14d)**

The title compound was isolated as a yellow solid (61%); ^{1}H NMR (400 MHz, MeOD) δ 8.08 (2H, d, *J* = 8.4 Hz), 7.76 (1H, d, *J* = 8.8 Hz), 7.47 (2H, d, *J* = 8.8 Hz), 7.40 (1H, d, *J* = 16.0 Hz), 7.09 (1H, d, *J* = 16.0 Hz), 6.96 (1H, d, *J* = 2.4 Hz), 6.88 - 6.85 (2H, m), 6.73 - 6.71 (2H, m); ^{13}C NMR (100 MHz, MeOD) δ 191.9, 163.6, 152.5, 149.9, 146.7, 146.6, 133.2, 130.0, 129.1, 127.9, 125.0, 123.4, 123.0, 116.4, 115.4, 114.4, 111.4; LRMS (ESI) calcd. for $C_{22}H_{16}O_6Cl$ $[M+H]^+$: 411.06, found : 411.10; HRMS (ESI) calcd. for $C_{22}H_{16}O_6Cl$ $[M+H]^+$: 411.0630, found : 411.0620; m.p. = 102.8 °C.

Supporting Information:

Acknowledgments

We acknowledge the generous financial support of the Gyeonggi provincial government.

Abbreviations used:

AUC, area under the curve; BA, bioavailability; CDT, complete decongestive therapy; Cl, chloride; Cmax, maximum concentration of a drug; DMEM, Dulbecco's modified Eagle's medium; DMF, dimethylformamide; F, fluorine; Fabp4, fatty acid-binding protein 4; FBS, fetal bovine serum; KOH, Potassium hydroxide; LOQ, the limit of quantitation; LPS, lipopolysaccharide; M-MLV, Moloney murine leukemia virus; MOM-Cl, methoxymethyl chloride; NSAID, nonsteroidal anti-inflammatory drug; OAc, acetoxy; OBz, benzoyl; O*i*Pr, isopropoxy; OMe, methoxy; PAMPA, parallel artificial membrane permeability assay; PPARγ, Peroxisome proliferator-activated receptor γ; RT-PCR, Real-time polymerase chain reaction; RVS, Rhus verniciflua Stokes; SAR, structure-activity relationship; $T_{1/2}$, terminal half-life; TNF-α, tumor necrosis factor α

References

1. Szuba, A.; Rockson, S. G. Lymphedema: classification, diagnosis and therapy. *Vascular medicine* **1998**, *3*, 145-156.

2. Rockson, S. G. Lymphedema. *The American journal of medicine* **2001**, *110*, 288-295.

3. Boyages, J.; Kalfa, S.; Xu, Y.; Koelmeyer, L.; Mackie, H.; Viveros, H.; Taksa, L.; Gollan, P. Worse and worse off: the impact of lymphedema on work and career after breast cancer. *Springerplus* **2016**, *5*, 657, doi:10.1186/s40064-016-2300-8.

4. Boris, M.; Weindorf, S.; Lasinski, B.; Boris, G. Lymphedema reduction by noninvasive complex lymphedema therapy. *Oncology* (Williston Park, NY) **1994**, *8*, 95-106; discussion 109 - 110.

5. Zampell, J. C.; Aschen, S.; Weitman, E. S.; Yan, A.; Elhadad, S.; Andrade, M. D. B.; Mehrara, B. J. Regulation of adipogenesis by lymphatic fluid stasis part I: adipogenesis, fibrosis, and inflammation. *Plast. Reconstr. Surg.* **2012**, *129*, 825-834.

6. Mak, S. S.; Yeo, W.; Lee, Y. M.; Mo, K. F.; Tse, K. Y.; Tse, S. M.; Ho, F. P.; Kwan, W. H. Predictors of lymphedema in patients with breast cancer undergoing axillary lymph node dissection in Hong Kong. *Nurs. Res.* **2008**, *57*, 416-425.

7. Tabibiazar, R.; Cheung, L.; Han, J.; Swanson, J.; Beilhack, A.; An, A.; Dadras, S. S.; Rockson, N.; Joshi, S.; Wagner, R.; Rockson, S. G. Inflammatory manifestations of experimental lymphatic insufficiency. *PLoS Med.* **2006**, *3*, e254.

8. Lin, S.; Kim, J.; Lee, M. J.; Roche, L.; Yang, N. L.; Tsao, P. S.; Rockson, S. G. Prospective transcriptomic pathway analysis of human lymphatic vascular insufficiency: identification and validation of a circulating biomarker panel. *PLoS One* **2012**, *7*, e52021.

9. Nishimura, S.; Manabe, I.; Nagasaki, M.; Eto, K.; Yamashita H.; Ohsugi, M.; Otsu, M.; Hara, K.; Ueki, K.; Sugiura, S.; Yoshimura, K.; Kadowaki, T.; Nagai, R. CD8 effector T cells contribute to macrophage recruitment and adipose tissue inflammation in obesity. *Nat. Med.* **2009**, *15*, 914–920.

10. Suganami, T.; Nishida, J.; Ogawa, Y. A paracrine loop between adipocytes and macrophages aggravates inflammatory changes: role of free fatty acids and tumor necrosis factor alpha. *Arterioscler. Thromb. Vasc. Biol.* **2005**, *25*, 2062–2068.

11. Swapna, G.; Daniel, A.; Cuzzone, J. S.; Torrisi, N. J.; Albano, W. J.; Joseph, I. L.; Savetsky, J. C.; Gardenier, D. C.; Jamie, C. Z.; Babak, J. M. Regulation of inflammation and fibrosis by macrophages in lymphedema. *Am. J. Physiol. Heart. Circ. Physiol.* **2015**, *308*, 1065–1077.

12. Leung, G.; Baggott, C.; West, C.; Elboim, C.; Paul, S. M.; Cooper, B. A.; Abrams, G.; Dhruva, A.; Schmidt, B. L.; Kober, K. Cytokine candidate genes predict the development of secondary lymphedema following breast cancer surgery. *Lymphat. Res. Biol.* **2014**, *12*, 10-22.

13. Ambus Jr, J. L.; Haneiwich, S.; Chesky, L.; McFarland, P.; Engler, R. J. Improved in vitro antigen-specific antibody synthesis in two patients with common variable immunodeficiency taking an oral cyclooxygenase and lipoxygenase inhibitor (ketoprofen). *J. Allergy Clin. Immunol.* **1991,** *88*, 775–783.

14. Gardenier, J. C.; Kataru, R. P.; Hespe, G. E.; Savetsky, I. L.; Torrisi, J. S.; Nores, G. D.; Jowhar, D. K.; Nitti, M. D.; Schofield, R. C.; Carlow, D. C.; Mehrara, B. J. Topical tacrolimus for the treatment of secondary lymphedema. *Nat. Commun.* **2017**, *8*, 14345, doi: 10.1038/ncomms14345.

15. Roh, K.; Kim, S.; Kang, H.; Ku, J.-M.; Park, K. W.; Lee, S. Sulfuretin has therapeutic activity against acquired lymphedema by reducing adipogenesis. *Pharmacol Res.* **2017**, *121*, 230-239.

16. Jung, C. H.; Kim, J.H.; Hong, M. H.; Seog, H. M.; Oh, S. H.; Lee, P. J.; Kim, G. J.; Um, J. Y.; Ko, S. G. Phenolic-rich fraction from Rhus verniciflua Stokes (RVS) suppress inflammatory response via NF-kappaB and JNK pathway in lipopolysaccharide-induced RAW 264.7 macrophages. *J. Ethnopharmacol.* **2007,** *110*, 490-497.

17. Song, N. J.; Yoon, H. J.; Kim, K. H.; Jung, S. R.; Jang, W. S.; Seo, C. R.; Lee, Y. M.; Kweon, D. H.; Hong, J. W.; Lee, J. S.; Park, K. M.; Lee, K. R.; Park, K. W. Butein is a novel anti-adipogenic compound. *J. Lipid Res.* **2013,** *54*, 1385-1396.

18. Lee, S.H.; Nan, J.X.; Zhao, Y.Z.; Woo, S.W.; Park, E.J.; Kang, T. H. The chalcone butein from Rhus verniciflua shows antifibrogenic activity. *Planta Med.* **2003,** *69*, 990-994.

19. Baell, J. B.; Holloway, G. A. New substructure filters for removal of pan assay interference compounds (PAINS) from screening libraries and for their exclusion in bioassays. *J. Med. Chem.* **2010**, *53*, 2719-2740.

20. Subbaiah, M. A. M.; Meanwell, N. A.; Kadow, J. Design strategies in the prodrugs of HIV-1 protease inhibitors to improve the pharmaceutical properties. *Eur. J. Med. Chem.* **2017,** *139*, 865-883.

21. Lv, P. C.; Elsayed, M. S.; Agama, K.; Marchand, C.; Pommier, Y.; Cushman, M. Design, Synthesis, and Biological Evaluation of Potential Prodrugs Related to the Experimental Anticancer Agent Indotecan (LMP400). *J. Med. Chem*. **2016**, *59*, 4890-4899.

22. Abonia, R.; Insuasty, D.; Castillo, J.; Insuasty, B.; Quiroga, J.; Nogueras, M.; Cobo, J. Synthesis of novel quinoline-2-one based chalcones of potential anti-tumor activity. *Eur. J. Med. Chem.* **2012**, *57*, 29-40.

23. Bhamabra, A.; Ruparelia, K. C.; Tan, H. L.; Tasdemir, D.; Burrell-Saward, H.; Yardley, V.; Beresford, K. J. M.; Arroo, R. R. J. Synthesis and antitrypanosomal activities of novel pyridylchalcones. *Eur. J. Med. Chem.* **2017**, *128*, 213-218.

24. Castano, L. F.; Cuartas, V.; Bernal, A.; Insuasty, A.; Guzman, J.; Vidal, O.; Rubio, V.; Pureto, G.; Lukac, P.; Vimberg, V.; Balikova-Notona, G.; Vannucci, L.; Janata, J.; Quiroga, J.; Abonia, R.; Nogueras, M.; Cobo, J.; Insuasty, B. New chalcone-sulfonamide hybrids exhibiting anticancer and antituberculosis activity. *Eur. J. Med. Chem.* **2019**, *176*, 50-60.

25. Ramya, R. V.; Guntuku, L.; Angapelly, S.; Digwal, C. S.; Lakshmi, U. J.; Sigalapalli, D. K.; Babu, B. N.; Naidu, V. G. M.; Kamal, A. Synthesis and biological evaluation of curcumin inspired imidazo[1,2-*a*]pyridine analogues as tubulin polymerization inhibitors. *Eur. J. Med. Chem.* **2018**, *143*, 216-231.

26. Bahekar, S.; Hande, S. V.; Agrawal, N. R.; Chandak, H. S.; Bhoj, P.; Goswami, K.; Reddy, M. V. R. Sulfonamide chalcones: Synthesis and *in vitro* exploration for therapeutic potential against *Brugia malayi*. *Eur. J. Med. Chem.* **2016**, *124*, 262-269.

27. Lee, J.-h.; Jeong, D.-Y.; Jung, S.-Y.; Lee, S.; Park, K. W.; Ku, J.-M. Cu(II) mediated chalcone synthesis via α-bromocarbonyl intermediate: A one step synthesis of echinatin. *Curr. Org. Chem.* **2017**, *21*, 652-658.

A

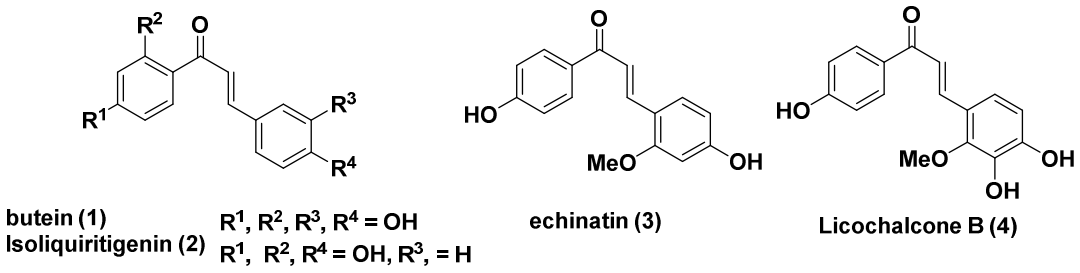

butein (1) $R^1, R^2, R^3, R^4 = OH$
Isoliquiritigenin (2) $R^1, R^2, R^4 = OH, R^3, = H$

echinatin (3)

Licochalcone B (4)

Figure 1. Chemical structure of compound **1** and its structurally related natural products..

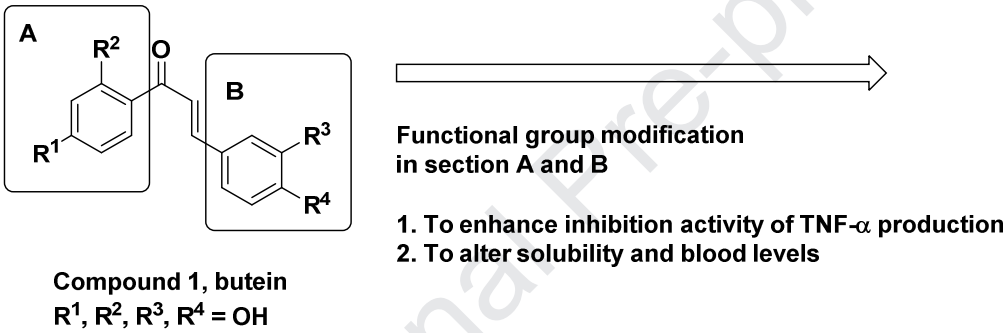

Compound 1, butein
$R^1, R^2, R^3, R^4 = OH$

Figure 2. Strategy of structural modification of compound **1.**.

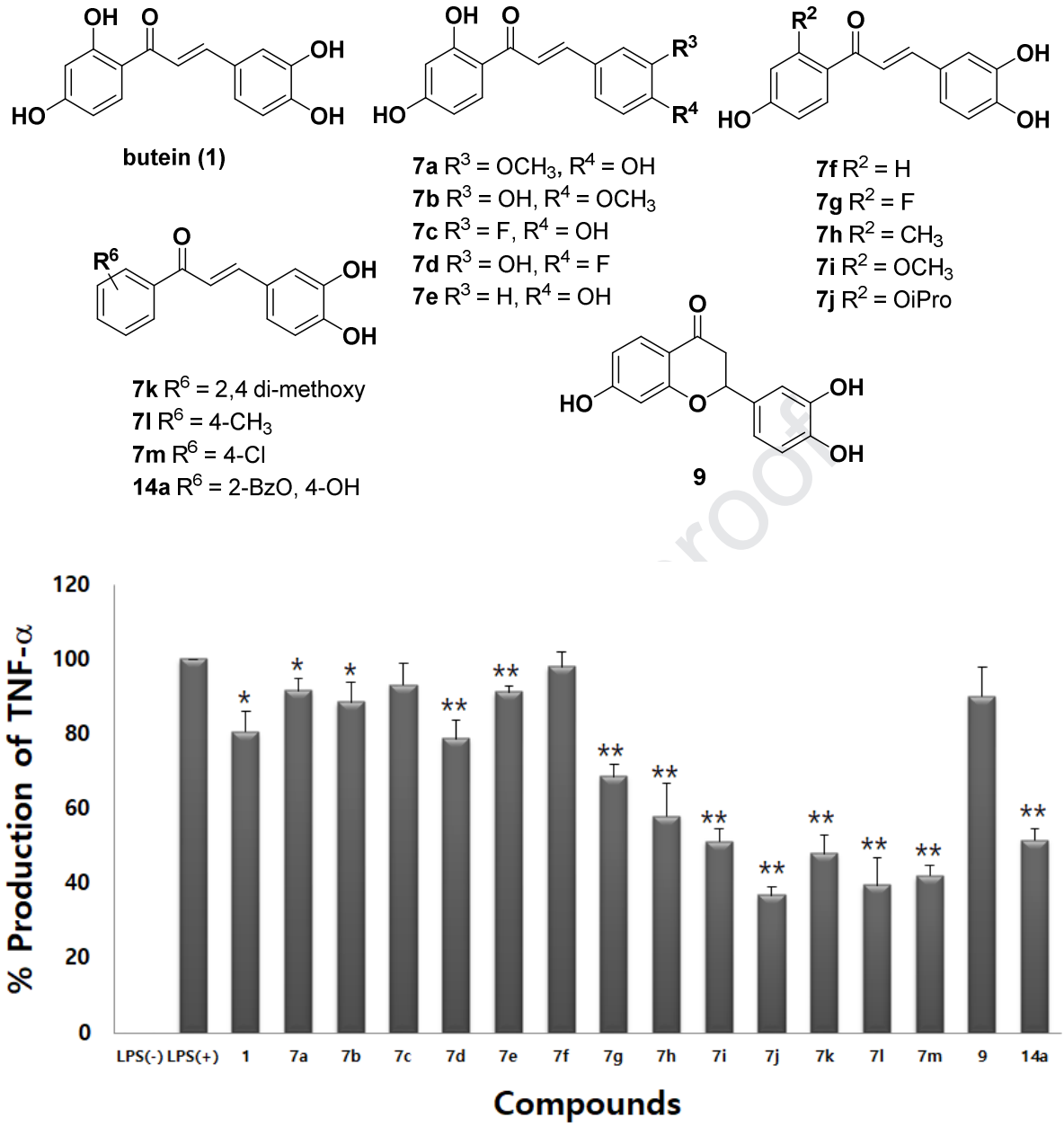

Figure 3. Compounds inhibiting LPS-induced TNF-α production in primary screening. Mouse peritoneal macrophages were stimulated with LPS in the presence of the indicated compounds (20 μM) for 24 h and the levels of TNF-α in supernatant were measured by ELISA. The data are shown as mean ± standard deviation, n = 3. * P<0.01, ** P<0.001 versus LPS(+).

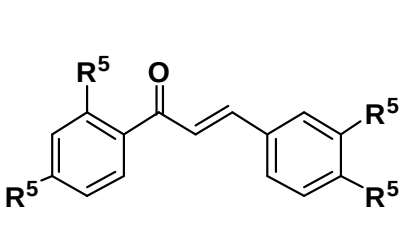

8a R = OAc
8b R = OBz

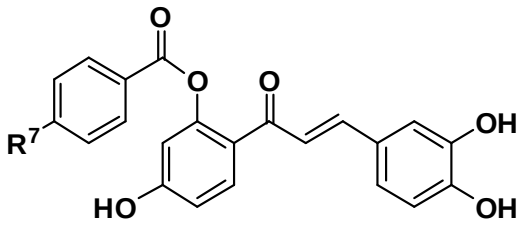

14a R^7 = H
14b R^7 = CH_3
14c R^7 = OCH_3
14d R^7 = Cl

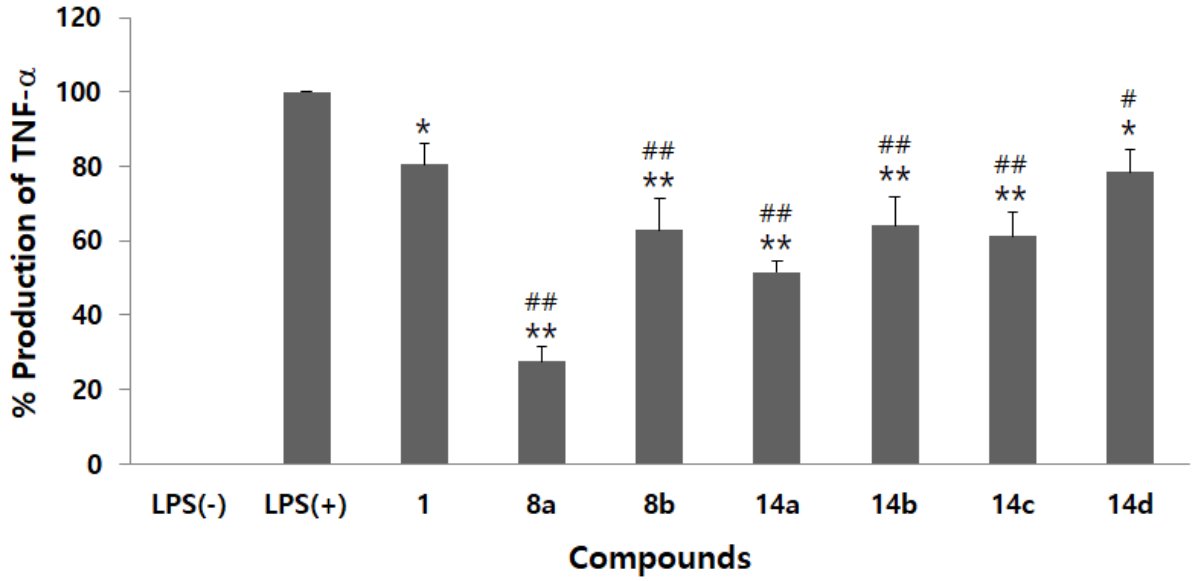

Figure 4. Compounds **14a-d** and **8a-b** inhibit LPS-induced TNF-α production. Mouse peritoneal macrophages were stimulated with LPS in the presence of the indicated compounds (20 μM) for 24 h and the levels of TNF-α in supernatant were measured by ELISA. The data are shown as mean ± standard deviation, n = 3. * P<0.01, ** P<0.001 versus LPS(+), # P<0.01, ## P<0.001 versus compound **1.**

Figure 5. Quantitation of limb volume on postsurgical day 7 for compound **1** and chemically modified derivatives (**7m** and **14a**). The normal group did not undergo surgery and the control and treatment groups (compounds **1** and **14a**) underwent surgery. Oral administration of compounds **1, 7m,** and **14a** to mice began seven days before the surgery and continued every two days after the surgery. Size of swelling in the right limb was measured on day seven post-surgery. * P<0.005 versus control; # P<0.001 versus compound **1.**

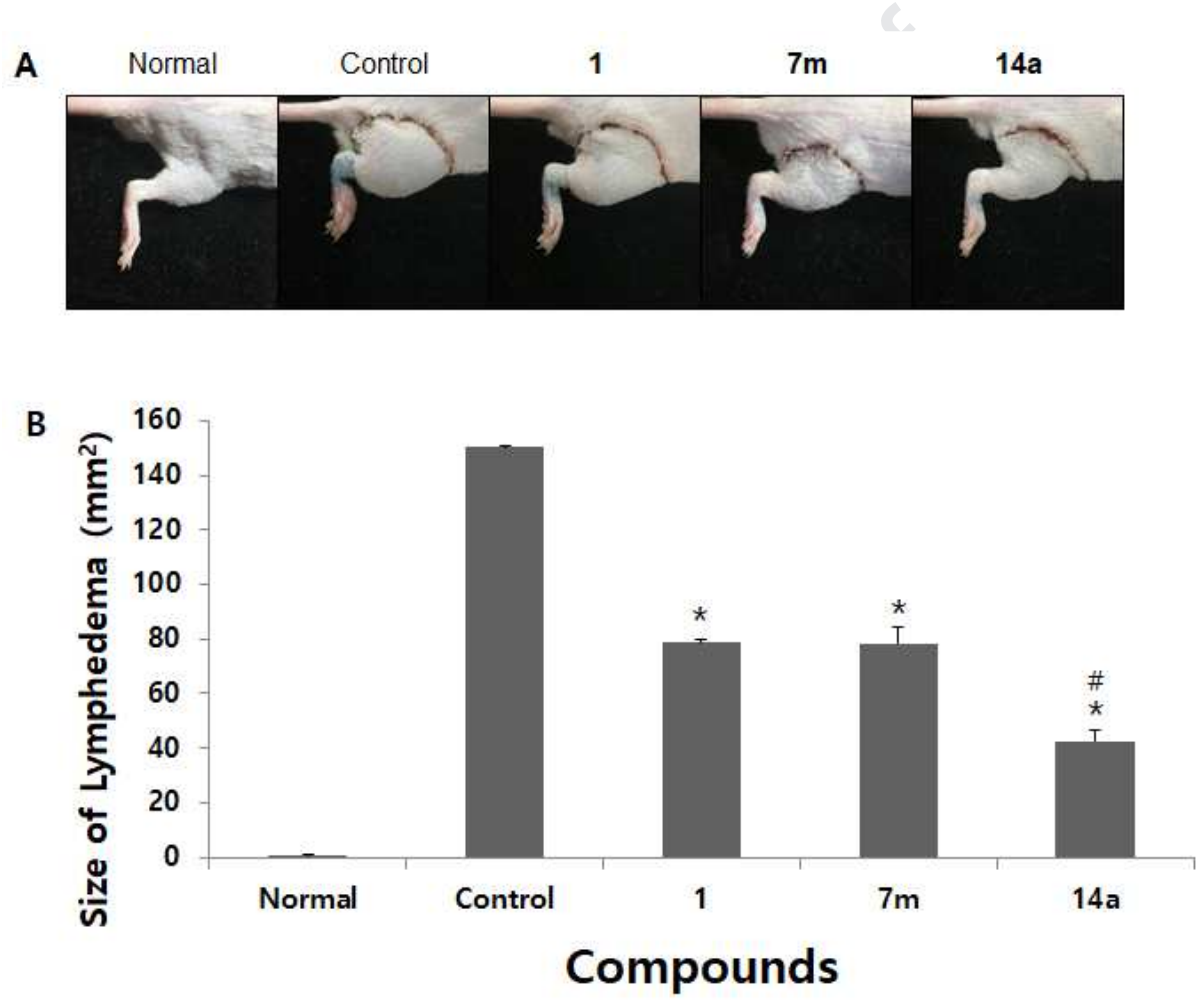

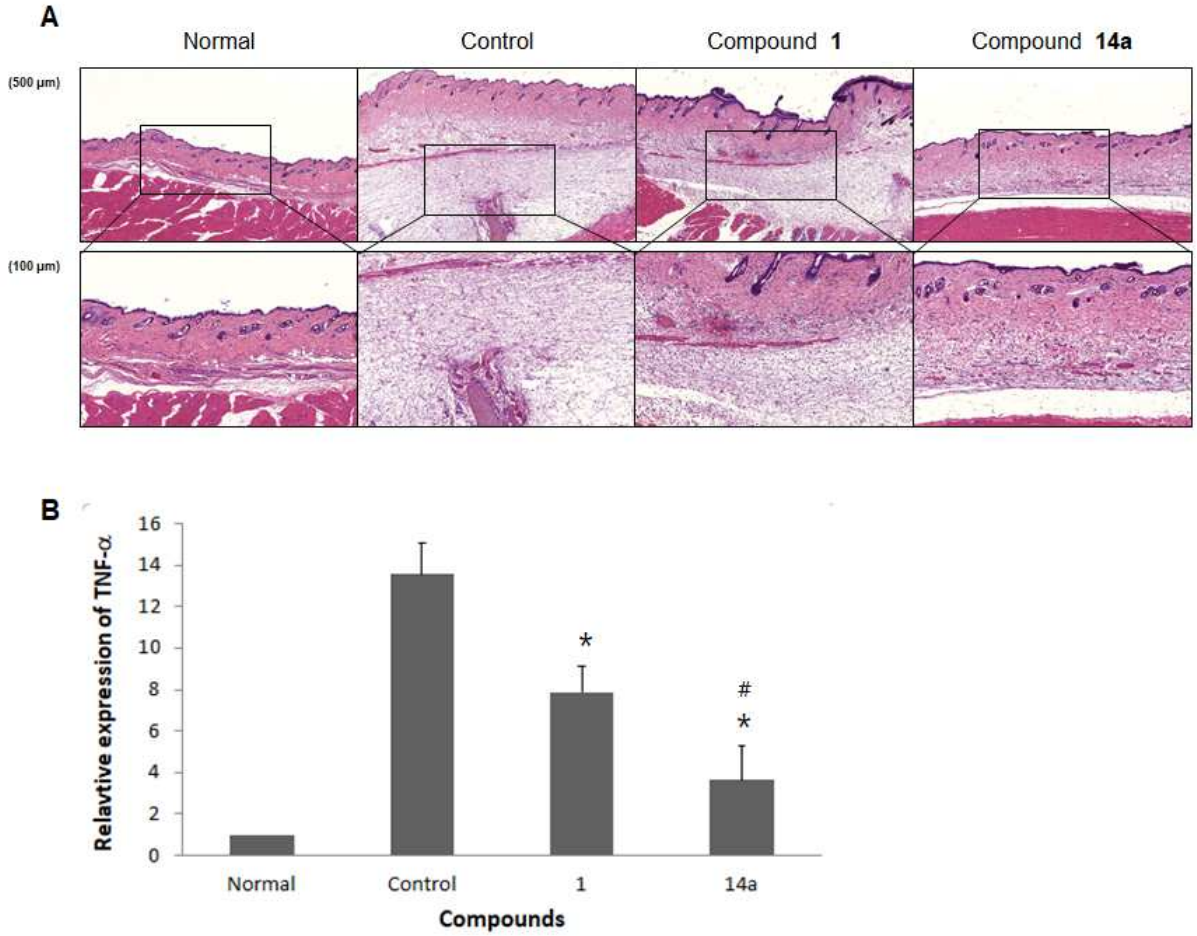

Figure 6. Compound **14a** reduces neutrophils and ameliorates lymphedema tissue in the dermal layer. (A) H&E images from the right hind limbs of mice in the normal group, lymphedema-induced vehicle-injected (control) group, compound **1**-treated group, and compound **14a**-treated group. Scale bar, 500 μm in upper panels and 100 μm in lower panels. (B) mRNA expression of TNF-α was assessed in each lymphedematous tissue. * $P<0.05$ versus control, # $P<0.05$ versus compound **1**.

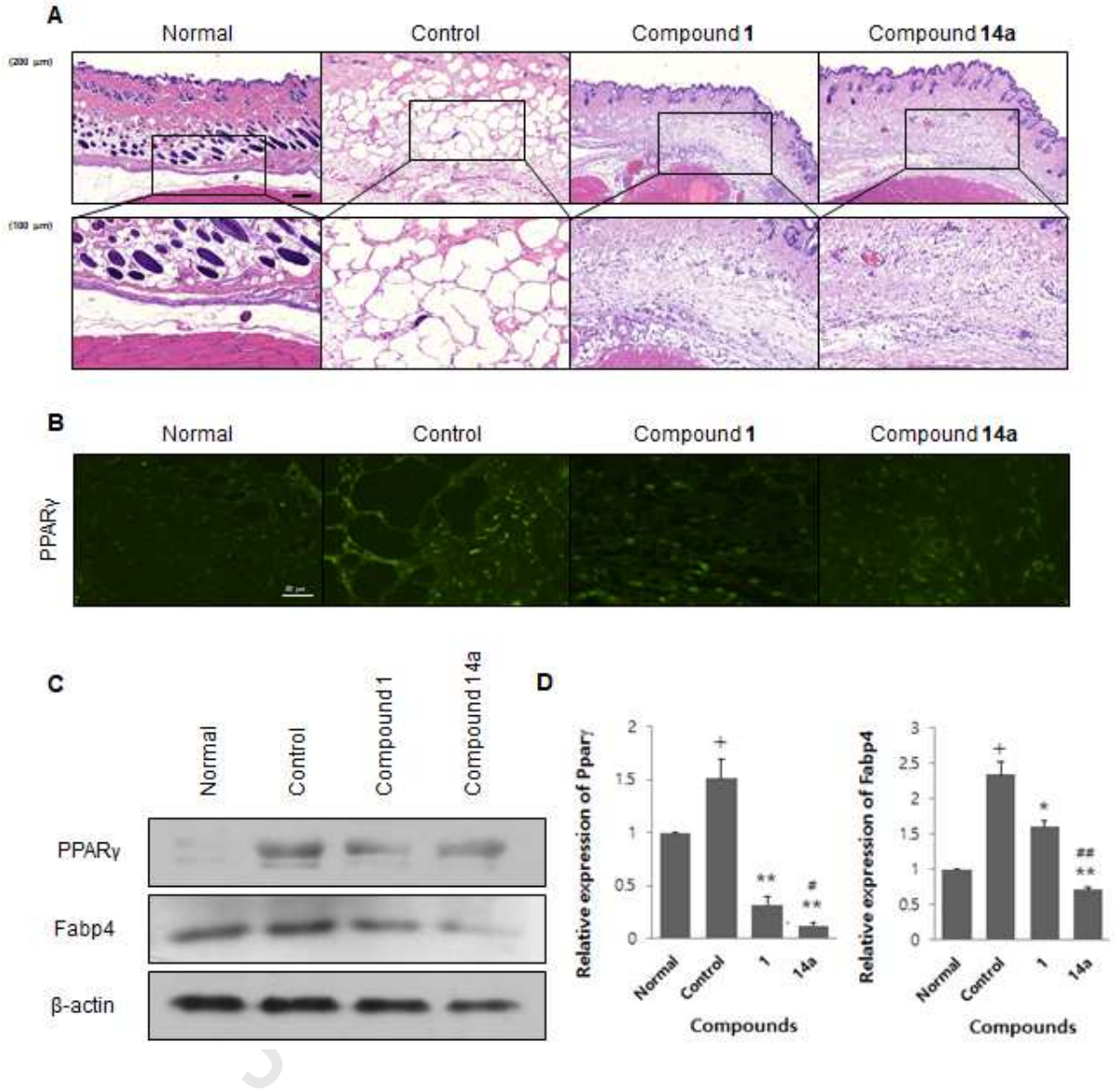

Figure 7. Compound **14a** has preventive effects on lymphedematous tissue via suppression of adipogenesis. (A) H&E images from the right hind limbs of mice in the normal group, lymphedema-induced vehicle-injected (control) group, compound **1**-treated group, and compound **14a**-treated group. Scale bar, 200 μm in upper panels and 50 μm in lower panels. (B) Representative images of immunofluorescence staining for PPARγ in lymphedematous tissue. (C) Protein expression of adipogenic biomarkers PPARγ and Fabp4 was assessed by western blotting. (D) Pparγ and Fabp4 mRNA levels in each group. + P<0.005 versus normal, * P<0.05, **<0.005 versus control, # P<0.01, ## P<0.001 versus compound **1**.

Scheme 1. Synthesis of compound **1** derivatives.

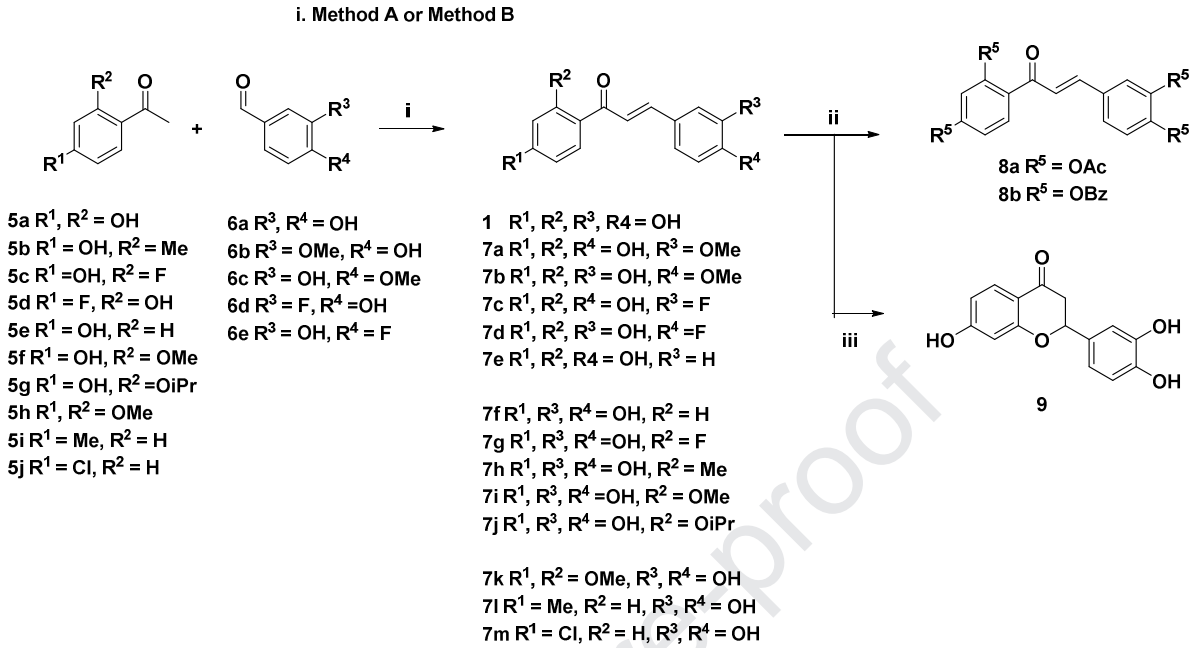

Reagents and conditions; (i) method A: 60% KOH(aq), ethanol, room temperature for 6 h, 60~72%; method B: 10% $CuBr_2$, ethyl acetate, 80 °C, 8 h, 42~60%; (ii) acetic anhydride, reflux, overnight, 93% or benzoyl chloride, TEA, THF, 6 h, 65%; (iii) KOH(s), methanol, reflux, 4 h, 60%.

Scheme 2. Synthesis of selective acylated compounds.

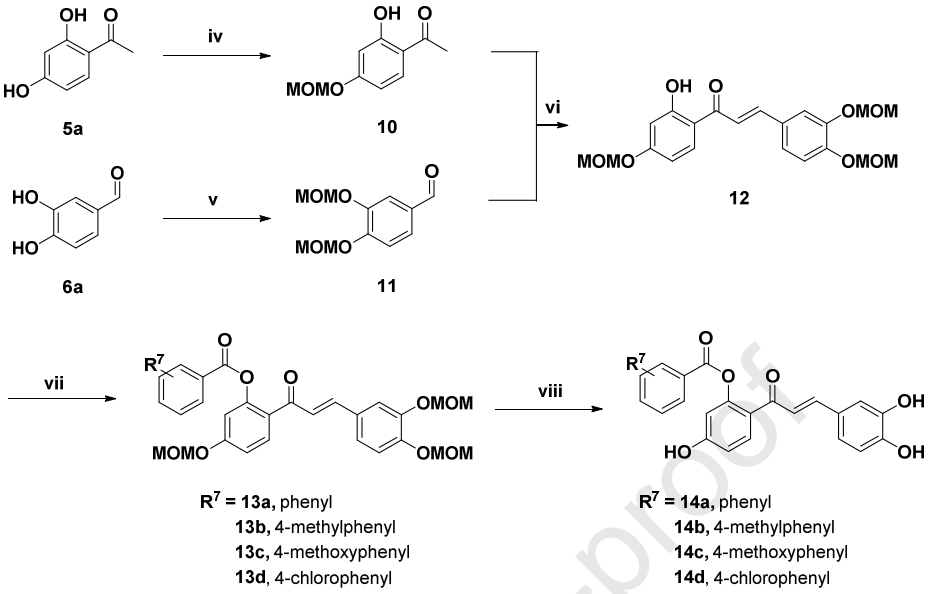

Reagents and conditions; (iv) methoxymethyl chloride, K_2CO_3, acetone, room temperature, 4 h, 61%; (v) methoxymethyl chloride, K_2CO_3, acetone, reflux, 2.5 h, 70%; (vi) 60% KOH(aq), ethanol, room temperature, 6 h, 70%; (vii) acyl chloride, TEA, DMF, room temperature, 2~3 h, 60~73%; (viii) 6N HCl(aq), ethanol, r.t, 4 h, 60 ~ 75%.

Table 1. Dose-dependent inhibition of LPS-induced TNF-α production in secondary screening.

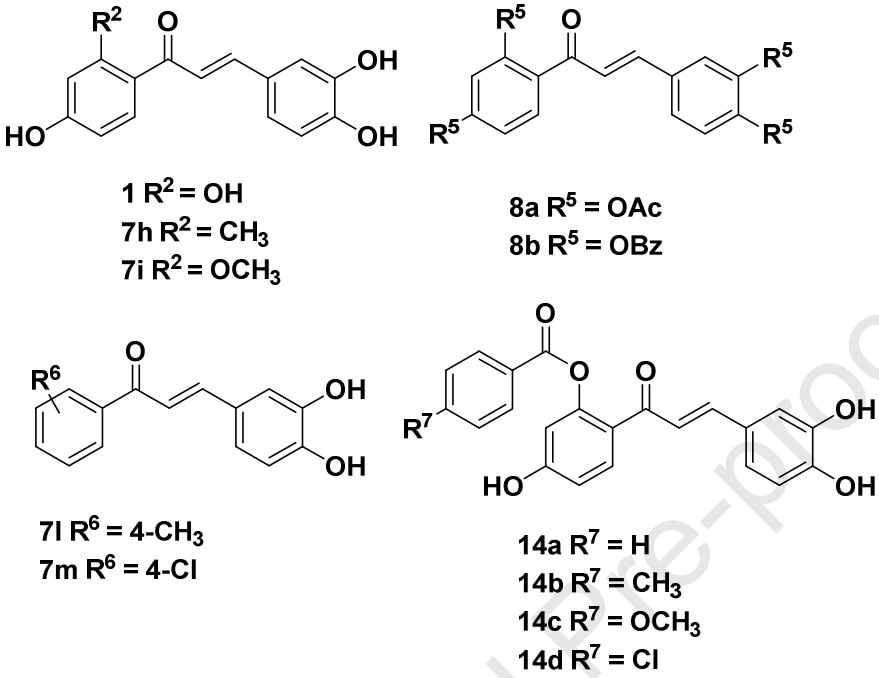

Entry	Compound	R	IC_{50}(μM)	Synthetic method
1	**1**	R^2 = OH	43.3 ± 1.72	A
2	**7h**	R^2 = CH_3	48.4 ± 2.35	B
3	**7i**	R^2 = OCH_3	32.2 ± 2.15	B
4	**7l**	R^6 = CH_3	18.6 ± 1.50	A
5	**7m**	R^6 = Cl	17.3 ± 2.11	A
6	**8a**	R^5 = OAc	12.8 ± 1.24	-
7	**8b**	R^5 = OBz	-	-
8	**14a**	R^7 = H	14.6 ± 1.56	A
9	**14b**	R^7 = CH_3	18.9 ± 1.15	A
10	**14c**	R^7 = OCH_3	20.8 ± 1.62	A
11	**14d**	R^7 = Cl	17.9 ± 1.84	A

[a]The data are shown as mean ± standard deviation, n = 2

Table 2. Physicochemical properties of compounds **1**, **7m**, and **14a**

Entry	Compound	pKa	logP	Permeability	Solubility
1	**1**	7.96/11.65	0.42	-5.35	21 μg/mL
2	**7m**	9.23/11.58	3.77	-4.33	28 μg/mL
3	**14a**	3.38/8.63/9.55	3.47	-5.67	136 μg/mL

Table 3. Liver microsomal stabilities of compounds **1**, **7m**, and **14a**

Entry	Compound	Compound remaining (%)		
		Mouse	Rat	Human
1	**1**	9.93	18.1	61.6
2	**7m**	7.26	21.1	38
3	**14a**	4	7	2
4	buspirone	0.0183	0.0928	4.7

[a]Metabolic stability was evaluated with remaining % of compounds 30 minutes after compounds were reacted in liver microsome.

[b]Buspirone, negative control, was metabolized in Phase I.

Table 4. Pharmacokinetic analysis of compounds **1**, and **14a**

Compound[a]	Administration route	Dose (mg/Kg)	$T_{1/2}$ (hr)	Tmax (hr)	Cmax (ng/mL)	AUCall (hr*ng/mL)	BA (%)
1	I.V	1		0.1	41	6.7	-
	P.O	20		0.3	43	21	15
	P.O	100		0.3	601	251	37
14a[b]	I.V	1	1.36	0.2	110	163	-

	P.O	20	0.57	0.4	83	141	4
	P.O	100	0.35	0.4	1600	1224	7.5

a Pre-formulation was achieved by 10% DMSO, 9% solutol in PBS.

b compound **1** as a primary metabolite of compound **14a** was analyzed to compare blood exposure of active ingredient.

$T_{1/2}$: terminal half-life. C_{max}: maximum plasma concentration. AUC_{∞}: area under the plasma concentration−time curve from time zero to infinity, indicating total blood exposure concentration. BA: bioavailability indicating $(AUC_{po}/AUC_{iv}) \times 100$.

The values of C_{max} and AUC_{∞} are the mean ± SD obtained from three male ICR mice.

1 Szuba, A.; Rockson, S. G. Lymphedema: classification, diagnosis and therapy. *Vascular medicine* **1998**, *3*, 145-156.

2 Rockson, S. G. Lymphedema. *The American journal of medicine* **2001**, *110*, 288-295.

3 Boyages, J.; Kalfa, S.; Xu, Y.; Koelmeyer, L.; Mackie, H.; Viveros, H.; Taksa, L.; Gollan, P. Worse and worse off: the impact of lymphedema on work and career after breast cancer. Springerplus **2016**, *5*, 657, doi:10.1186/s40064-016-2300-8.

4 Boris, M.; Weindorf, S.; Lasinski, B.; Boris, G. Lymphedema reduction by noninvasive complex lymphedema therapy. *Oncology* (Williston Park, NY) **1994**, *8*, 95-106; discussion 109 - 110.

5 Zampell, J. C.; Aschen, S.; Weitman, E. S.; Yan, A.; Elhadad, S.; Andrade, M. D. B.; Mehrara, B. J. Regulation of adipogenesis by lymphatic fluid stasis part I: adipogenesis, fibrosis, and inflammation. *Plast. Reconstr. Surg.* **2012**, *129*, 825-834.

6 Mak, S. S.; Yeo, W.; Lee, Y. M.; Mo, K. F.; Tse, K. Y.; Tse, S. M.; Ho, F. P.; Kwan, W. H. Predictors of lymphedema in patients with breast cancer undergoing axillary lymph node dissection in Hong Kong. *Nurs. Res.* **2008**, *57*, 416-425.

7 Tabibiazar, R.; Cheung, L.; Han, J.; Swanson, J.; Beilhack, A.; An, A.; Dadras, S. S.; Rockson, N.; Joshi, S.; Wagner, R.; Rockson, S. G. Inflammatory manifestations of experimental lymphatic insufficiency. *PLoS Med.* **2006**, *3*, e254.

8 Lin, S.; Kim, J.; Lee, M. J.; Roche, L.; Yang, N. L.; Tsao, P. S.; Rockson, S. G. Prospective transcriptomic pathway analysis of human lymphatic vascular insufficiency: identification and validation of a circulating biomarker panel. *PLoS One* **2012**, *7*, e52021.

9 Nishimura, S.; Manabe, I.; Nagasaki, M.; Eto, K.; Yamashita H.; Ohsugi, M.; Otsu, M.; Hara, K.; Ueki, K.; Sugiura, S.; Yoshimura, K.; Kadowaki, T.; Nagai, R. CD8 effector T cells contribute to macrophage recruitment and adipose tissue inflammation in obesity. *Nat. Med.* **2009**, *15*, 914–920.

10 Suganami, T.; Nishida, J.; Ogawa, Y. A paracrine loop between adipocytes and macrophages aggravates inflammatory changes: role of free fatty acids and tumor necrosis factor alpha. *Arterioscler. Thromb. Vasc. Biol.* **2005**, *25*, 2062–2068.

11 Swapna, G.; Daniel, A.; Cuzzone, J. S.; Torrisi, N. J.; Albano, W. J.; Joseph, I. L.; Savetsky, J. C.; Gardenier, D. C.; Jamie, C. Z.; Babak, J. M. Regulation of inflammation and fibrosis by macrophages in lymphedema. *Am. J. Physiol. Heart. Circ. Physiol.* **2015**, *308*, 1065–1077.

12 Leung, G.; Baggott, C.; West, C.; Elboim, C.; Paul, S. M.; Cooper, B. A.; Abrams, G.; Dhruva, A.; Schmidt, B. L.; Kober, K. Cytokine candidate genes predict the development of secondary lymphedema following breast cancer surgery. *Lymphat. Res. Biol.* **2014**, *12*, 10-22.

13 Ambus Jr, J. L.; Haneiwich, S.; Chesky, L.; McFarland, P.; Engler, R. J. Improved in vitro antigen-specific antibody synthesis in two patients with common variable immunodeficiency taking an oral cyclooxygenase and lipoxygenase inhibitor (ketoprofen). *J. Allergy Clin. Immunol.* **1991,** *88*, 775–783.

14 Gardenier, J. C.; Kataru, R. P.; Hespe, G. E.; Savetsky, I. L.; Torrisi, J. S.; Nores, G. D.; Jowhar, D. K.; Nitti, M. D.; Schofield, R. C.; Carlow, D. C.; Mehrara, B. J. Topical tacrolimus for the treatment of secondary lymphedema. *Nat. Commun.* **2017**, *8*, 14345, doi: 10.1038/ncomms14345.

15 Roh, K.; Kim, S.; Kang, H.; Ku, J.-M.; Park, K. W.; Lee, S. Sulfuretin has therapeutic activity against acquired lymphedema by reducing adipogenesis. *Pharmacol Res.* **2017**, *121*, 230-239.

16 Jung, C. H.; Kim, J.H.; Hong, M. H.; Seog, H. M.; Oh, S. H.; Lee, P. J.; Kim, G. J.; Um, J. Y.; Ko, S. G. Phenolic-rich fraction from Rhus verniciflua Stokes (RVS) suppress inflammatory response via NF-kappaB and JNK pathway in lipopolysaccharide-induced RAW 264.7 macrophages. *J. Ethnopharmacol.* **2007,** *110*, 490-497.

17 Song, N. J.; Yoon, H. J.; Kim, K. H.; Jung, S. R.; Jang, W. S.; Seo, C. R.; Lee, Y. M.; Kweon, D. H.; Hong, J. W.; Lee, J. S.; Park, K. M.; Lee, K. R.; Park, K. W. Butein is a novel anti-adipogenic compound. *J. Lipid Res.* **2013,** *54*, 1385-1396.

18 Lee, S.H.; Nan, J.X.; Zhao, Y.Z.; Woo, S.W.; Park, E.J.; Kang, T. H. The chalcone butein from Rhus verniciflua shows antifibrogenic activity. *Planta Med.* **2003,** *69*, 990-994.

19 Baell, J. B.; Holloway, G. A. New substructure filters for removal of pan assay interference compounds (PAINS) from screening libraries and for their exclusion in bioassays. J. Med. Chem. **2010**, *53*, 2719-2740.

20 Subbaiah, M. A. M.; Meanwell, N. A.; Kadow, J. Design strategies in the prodrugs of HIV-1 protease inhibitors to improve the pharmaceutical properties. *Eur. J. Med. Chem.* **2017,** *139*, 865-883.

21 Lv, P. C.; Elsayed, M. S.; Agama, K.; Marchand, C.; Pommier, Y.; Cushman, M. Design, Synthesis, and Biological Evaluation of Potential Prodrugs Related to the Experimental Anticancer Agent Indotecan (LMP400). *J. Med. Chem*. **2016**, *59*, 4890-4899.

22 Abonia, R.; Insuasty, D.; Castillo, J.; Insuasty, B.; Quiroga, J.; Nogueras, M.; Cobo, J. Synthesis of novel quinoline-2-one based chalcones of potential anti-tumor activity. *Eur. J. Med. Chem.* **2012**, *57*, 29-40.

23 Bhamabra, A.; Ruparelia, K. C.; Tan, H. L.; Tasdemir, D.; Burrell-Saward, H.; Yardley, V.; Beresford, K. J. M.; Arroo, R. R. J. Synthesis and antitrypanosomal activities of novel pyridylchalcones. *Eur. J. Med. Chem.* **2017**, *128*, 213-218.

24 Castano, L. F.; Cuartas, V.; Bernal, A.; Insuasty, A.; Guzman, J.; Vidal, O.; Rubio, V.; Pureto, G.; Lukac, P.; Vimberg, V.; Balikova-Notona, G.; Vannucci, L.; Janata, J.; Quiroga, J.; Abonia, R.; Nogueras, M.; Cobo, J.; Insuasty, B. New chalcone-sulfonamide hybrids exhibiting anticancer and antituberculosis activity. *Eur. J. Med. Chem*. **2019**, *176*, 50-60.

25 Ramya, R. V.; Guntuku, L.; Angapelly, S.; Digwal, C. S.; Lakshmi, U. J.; Sigalapalli, D. K.; Babu, B. N.; Naidu, V. G. M.; Kamal, A. Synthesis and biological evaluation of curcumin inspired imidazo[1,2-*a*]pyridine analogues as tubulin polymerization inhibitors. *Eur. J. Med. Chem*. **2018**, *143*, 216-231.

26 Bahekar, S.; Hande, S. V.; Agrawal, N. R.; Chandak, H. S.; Bhoj, P.; Goswami, K.; Reddy, M. V. R. Sulfonamide chalcones: Synthesis and *in vitro* exploration for therapeutic potential against *Brugia malayi*. *Eur. J. Med. Chem*. **2016**, *124*, 262-269.

27 Lee, J.-h.; Jeong, D.-Y.; Jung, S.-Y.; Lee, S.; Park, K. W.; Ku, J.-M. Cu(II) mediated chalcone synthesis via α-bromocarbonyl intermediate: A one step synthesis of echinatin. *Curr. Org. Chem.* **2017**, *21*, 652-658.

Highlights

Inflammation affects progression of acquired lymphedema.

The compounds 8s and 14s significantly showed anti-inflammatory activity in vitro.

The compound 14a suppressed limb volume by 70% compared to control in animal model.

Enhancing blood level of active ingredient improved suppression of lymphedema.

Declaration of interests

☒ The authors declare that they have no known competing financial interests or personal relationships that could have appeared to influence the work reported in this paper.

☐The authors declare the following financial interests/personal relationships which may be considered as potential competing interests: